

STATOR INTER TURN SHORT CIRCUIT FAULT DIAGNOSIS IN THREE PHASE INDUCTION MOTOR USING NEURAL NETWORKS

Prachi Sinhal
111ee0053



Department of Electrical Engineering
National Institute of Technology Rourkela

STATOR INTER TURN SHORT CIRCUIT FAULT DIAGNOSIS IN THREE PHASE INDUCTION MOTOR USING NEURAL NETWORKS

*Thesis submitted in partial fulfillment
of the requirements for the degree of*

Bachelor of Technology

In

Electrical Engineering

By

Prachi Sinhal

Roll No. 111ee0053

Under the guidance of

Prof. Bidyadhar Subudhi



**Department of Electrical Engineering
National Institute of Technology Rourkela**



**Department of Electrical Engineering
National Institute of Technology, Rourkela**

Certificate

*This is to certify that the thesis entitled, “STATOR INTER TURN SHORT CIRCUIT FAULT DIAGNOSIS IN THREE PHASE INDUCTION MOTOR USING NEURAL NETWORKS” submitted by Prachi Sinhal in partial fulfillment of the requirements for the award of **Bachelor of Technology Degree in Electrical Engineering** at National Institute of Technology, Rourkela is an veritable work carried out by her under my supervision and guidance. To the best of my knowledge, the matter embodied in this Project review report has not been submitted to any other university or institute for award of any Degree or Diploma.*

Prof. Bidyadhar Subudhi
Department of Electrical Engineering
National Institute of Technology, Rourkela

Place: Rourkela

Date:

Acknowledgement

I take the chance to express my adoration to my director Prof. Bidyadhar Subudhi for his direction, motivation and inventive specialized examinations over the span of this work. His unending vitality and energy in examination had propelled others, including me. Likewise, he was constantly open and willing to help his understudies with their examination. Subsequently, investigate life got to be smooth and remunerating for me.

I thank all my teachers Prof. A.K. Panda, Prof. D. Patra, Prof. K. R. Subhashini, Prof P K Ray, Prof S. Gopala Krishna, Prof S. Maity, Prof S. Ghosh, Prof S. Ganguly, Prof M. Pattanaik, Prof S.P. Gupta and Prof S. Das for their contribution in my studies and research work. They have been incredible wellsprings of motivation to me and I express gratitude toward them in the name of all that is holy.

I would like to express my thanks to Mr. S. Swain for helping me for conducting my experimental work.

I might want to thank every one of my companions and particularly my cohorts for all the insightful and psyche fortifying exchanges we had, which incited us to think past the self-evident.

To wrap things up I might want to thank my guardians, who taught me the estimation of diligent work by their own case. They rendered me colossal backing being separated amid the entire residency of my stay in NIT Rourkela.

Prachi Sinhal

CONTENTS

Abstract	vii
List of Tables	viii
List of Figures	ix
Acronyms	xi
1 Introduction	
1.1 Background	1
1.2 Literature Review on Fault Diagnosis of Induction Motor	1
1.3 Different Types of Faults in an Induction Motor	4
1.4 Motivation	5
1.5 Objectives of the Thesis	5
1.6 Organization of the Thesis	6
2 Experimental Setup and Data Generation for Induction Motor	
Fault Diagnosis	
2.1 Experimental Setup	7
2.2 Data generation through experiment	8
2.3 Assumptions made	11
2.4 Chapter Summary	13
3 Different Artificial Neural Network Techniques	
3.1 Introduction	14
3.2 Chapter Objectives	14
3.3 Multilayer Perceptron Neural Network	14
3.3.1 Back Propagation Algorithm (BPA)	15
3.3.2 Flow chart for Back Propagation Algorithm	17

3.4 Radial Basis Function Neural Network	18
3.4.1 Commonly used Radial Basis Functions	18
3.4.2 Typical Radial Basis Function that has been used for the simulation	19
3.4.3 Flow chart for Radial Basis Function Neural Network	21
3.5 Training Methodology of the Neural Networks	22
3.6 Chapter Summary	22
4 Data Generation from the Simulated Neural Networks	
4.1 Introduction	23
4.2 Simulation Set-up	23
4.3 Results of Simulation of Back Propagation Algorithm	23
4.4 Results of Simulation of Radial Basis Function Neural Network	30
4.5 Comparison between RBFNN and BPA	34
4.6 Chapter Summary	35
5 Short Circuit Inter Turn Fault Diagnosis using Discrete Wavelet Transform	
5.1 Introduction	36
5.2 Chapter Objectives	36
5.3 Discrete Wavelet Transform	35
5.4 Methodology adopted to implement DWT for Fault Diagnosis of Induction Motor	38
5.5 Results and Discussions	39
5.5.1 Tabulation of approximate RMS error in the coefficients for different l and m obtained from RBFNN	41
5.6 Chapter Summary	46
6 Conclusions and Suggestions for Future Work	
6.1 Conclusions of the Thesis	47
6.2 Thesis Contributions	48
6.3 Future scope of work	49

ABSTRACT

In induction machine a number of faults occur namely bearing and insulation related faults, stator winding and rotor related faults. Among these, stator inter-turn fault is one of the most common faults which occur due to ageing effect, contaminated lubricants, excessive loading, non-uniformity of magnetic field, excess radial or axial forces, partial short circuit in the windings, radial or axial misalignment between the motor and load, bearing currents etc. Therefore, this work deals with the diagnosis of inter turn short circuit fault in stator winding of an induction machine. These incipient faults need to be identified and cleared as soon as possible to reduce failures as well as maintenance cost. Conventional methods are time taking and require exact mathematical modelling of the machine. However, due to ageing effects the mathematical model has to be modified from time to time so that one can employ soft computing methods which are suitable in the situation where dynamics of the system is less understood such as the fault dynamics of an induction machine.

In this thesis, one of the very popular soft computing techniques called artificial neural network is employed to diagnose the stator inter turn short-circuit fault in a three phase squirrel cage induction machine. Firstly, a multilayer perceptron neural network (MLPNN) has been applied for solving the above fault diagnosis problem. In order to apply multilayer perceptron artificial neural network for fault diagnosis, an induction machine in the lab is considered. Three phase variable AC voltage is applied to induction machine through a three phase variac and the stator line voltage and stator currents were measured for both healthy and faulted motor. Then a multilayer perceptron neural network was developed with 3 layers namely input, hidden and output layer with 2 nodes in input and output layer whereas four nodes in the hidden layer. Using the stator line voltage and stator currents, back propagation algorithm is employed to train the said MLPNN. The root mean square error was plotted and the least value was found to be 0.065. In view of improving the training performance, a radial basis function neural network (RBFNN) with the same configuration as that of back propagation algorithm and Discrete Wavelet Transform was designed. Then the results of both the artificial neural networks and DWT were compared and it was found that RBFNN outperforms both the MLPNN and DWT based fault diagnosis approaches applied to the induction machine.

LIST OF TABLES

- Table I Induction motor ratings
- Table II Induction motor readings under healthy condition
- Table III Induction motor readings under faulty condition
- Table IV Normalized data of phase R
- Table V Obtained condition of healthiness using BPA for $l=0.1$, $m=0.4$ and $m=0.5$
- Table VI Obtained condition of healthiness using BPA for $m=0.5$, $l=0.2$ and $l=0.3$
- Table VII Obtained condition of healthiness using BPA for $m=0.4$, $l=0.1$ and $l=0.2$
- Table VIII Obtained approximate root mean square error using RBFNN for $l=0.1$,
 $m=0.4$ and $m=0.5$
- Table IX Obtained approximate root mean square error using RBFNN
for $m=0.4$, $l=0.2$ and $l=0.3$
- Table X Obtained approximate root mean square error using RBFNN
for $m=0.5$, $l=0.2$ and $l=0.3$
- Table XI Comparison of root mean square error obtained in case of BPA and RBFNN
- Table XII Detailed and approximation coefficients for input and output samples
- Table XIII Approximate RMS error in the coefficients for $l=0.1$, $m=0.4$ and $m=0.5$
- Table XIV Approximate RMS error in the coefficients for $m=0.5$, $l=0.2$ and $l=0.3$
- Table XV Approximate RMS error in the coefficients for $m=0.4$, $l=0.1$ and $l=0.2$
- Table XVI RMS error in case of BPA, RBFNN and DWT

LIST OF FIGURES

- 2.1 Block diagram of experimental set-up
- 2.2 Experimental Setup of a 3 phase 2 hp Induction Motor connected to variac at no load
- 2.3 Stator Winding Turn 1 to (N/7) Shorted
- 2.4 Stator Winding Turn 1 to (3N/7) Shorted
- 3.1 Configuration of Multilayer Perceptron Neural Network
- 4.1 Root mean square error in the healthiness of insulation condition for $l=0.1$, $m=0.4$ using BPA
- 4.2 Root mean square error in the healthiness of insulation condition for $l=0.1$, $m=0.5$ using BPA
- 4.3 Root mean square error in the healthiness of insulation condition for $l=0.2$, $m=0.5$ using BPA
- 4.4 Root mean square error in the healthiness of insulation condition for $l=0.3$, $m=0.5$ using BPA
- 4.5 Root mean square error in the healthiness of insulation condition for $l=0.1$, $m=0.4$ using BPA
- 4.6 Root mean square error in the healthiness of insulation condition for $l=0.2$, $m=0.4$ using BPA
- 4.7 Root mean square error in the healthiness of insulation condition for $l=0.1$, $m=0.4$
using RBFNN
- 4.8 Root mean square error in the healthiness of insulation condition for $l=0.1$, $m=0.5$
using RBFNN
- 4.9 Root mean square error in the healthiness of insulation condition for $l=0.2$, $m=0.4$
using RBFNN
- 4.10 Root mean square error in the healthiness of insulation condition for $l=0.3$, $m=0.4$
using RBFNN
- 4.11 Root mean square error in the healthiness of insulation condition for $l=0.2$, $m=0.5$
using RBFNN
- 4.12 Root mean square error in the healthiness of insulation condition for $l=0.3$, $m=0.5$
using RBFNN
- 5.1 Block diagram of DWT
- 5.2 RMS error vs. no of iterations in detailed and approximation coefficients of target output
for $l=0.1$ and $m=0.4$

5.3 RMS error vs. no of iterations in detailed and approximation coefficients of target output
for $l=0.1$ and $m=0.5$

5.4 RMS error vs. no of iterations in detailed and approximation coefficients of target output
for $l=0.2$ and $m=0.5$

5.5 RMS error vs. no of iterations in detailed and approximation coefficients of target output
for $l=0.3$ and $m=0.5$

5.6 RMS error vs. no of iterations in detailed and approximation coefficients of target output
for $l=0.1$ and $m=0.4$

5.7 RMS error vs. no of iterations in detailed and approximation coefficients of target output
for $l=0.2$ and $m=0.4$

ACRONYMS

BPA:	Back propagation algorithm
RBFNN:	Radial basis function neural network
MLPNN:	Multi layer perceptron neural network
RBF:	Radial basis function
l:	Learning rate
m:	Momentum rate
DWT:	Discrete wavelet transform
WT:	Wavelet transform
RMS:	Root mean square
MRA:	Multi-resolution analysis
CQFs:	Conjugate quadrature filters
BDWT:	Biorthogonal discrete wavelet transform
DCT:	Discrete cosine transform
WNN:	Wavelet neural network

Chapter 1

Introduction

1.1 Background

Induction motors are most widely used in industries as well as for domestic purposes because they are highly reliable, robust, and economical and require least maintenance. However due to change in loading conditions and working environment they are subjected to certain wear and tear which may lead to incipient faults, which if not identified and cleared will lead to complete failure of the machine. So the faults need to be diagnosed as soon as possible which will save maintenance cost as well as prevent failures. Thus fault diagnosis in induction motors is one of the challenging topic.

Recently soft computing techniques such as expert system, neural network, fuzzy logic, adaptive neural fuzzy inference system, genetic algorithm etc. are used for the diagnosis of faulty conditions. These techniques have gained popularity over other conventional techniques. These are easy to apply and modify besides their improved performance. The neural system can represent any non-direct model without having the points of interest of the genuine structure and can give bring about a brief while. From the early phases of creating electrical machines, analysts have been occupied with building up a system for machine examination, security and upkeep. The utilization of above strategy expands the exactness and precision of the checking frameworks. The range of condition observing and flaws indicative of electrical drives is basically identified with various subjects, for example, electrical machines, routines for checking, unwavering quality and upkeep, instrumentation, sign preparing and astute frameworks.

1.2 Literature Review on Fault Diagnosis of Induction Motor

Mo-Yuen Chow, Peter M.Mangum and Sui Oi Yee [1] designed neural network for incipient fault detection in $\frac{3}{4}$ -hp permanent magnet induction motor. He designed a satisfactory method using neural network approach from which the healthiness of the machine can be accessed and it can be

applied for small and medium sized induction motors with 95% satisfactory result.

James E. Timperly [3] proposed a method for diagnosis of incipient fault by monitoring electromagnetic interference. This method detected stator deterioration as well as design defects. Wide band spectrum analysis indicated the location of fault, machine healthiness and fault location.

Thomson and Fenger [5] have used the current signature analysis technique to detect the induction machine faults. This technique uses the motor current signature to detect the different faults in squirrel cage induction motor, detection of shorted turns in an induction motor. In this paper the author has taken four case studies which is used to detect the different faults in an induction motors. From the results the author has clearly demonstrated that the motor current signature analysis is a powerful technique for monitoring the health of three phase induction motors.

Nejjari and Benbouzid [6] have utilized the Park's vector designs for distinguishing diverse sorts of supply blames, for example, voltage irregularity and single staging. Notwithstanding this based back spread calculation is utilized to acquire the machine condition by testing the state of the Park's vector designs. Two neural system based methodology has been utilized, these are established and decentralized. The all-inclusive statement of the proposed approach has been tentatively tried and the creator asserts that the outcomes give an agreeable level of exactness.

Yousef Akhlaghi [9] says that Radial Basis Function Networks are a special class of single hidden layer feed forward neural networks for application to problems of supervised learning. He says that Radial Basis Function Neural Network models are non-parametric and their weights and other parameters have no particular meaning in relation to the problems to which they are applied, its primary goal is to estimate the output at certain desired values of the input. He calculates the RBFNN parameters like the centers, spreads and the weights. He uses the forward selection and the backward elimination process and then he orthonormalizes the basis function.

H.A Talebi and Farzaneh Abdollahi [10] classify the commonly used radial basis functions and

define the localization of the Gaussian function. They explain the process of center selection in RBFNN, K-Mean Clustering and show the steps involved in finding the output weights.

Fillipetti [11] has presented an exhaustive study about the use of computerized reasoning in machine checking and deficiency conclusion. Here, master framework has been utilized as a instrument for the shortcoming conclusion. The creators demonstrate the legitimacy of utilizing neural system alongside fluffy rationale for issue recognizable proof and flaw seriousness assessment. The paper additionally covers a judgment of the inverter framework, which is utilized to drive the machine.

Zwe-Lee Gaing [12] executed a model wavelet-based neural system classifier for perceiving force quality unsettling influences and tried under different transient occasions. The discrete wavelet change (DWT) procedure is coordinated with the probabilistic neural-system (PNN) model to develop the classifier. The multi determination investigation strategy of DWT and the Parseval's hypothesis are utilized to concentrate the vitality dissemination highlights of the contorted sign at diverse determination levels. Since the proposed technique can lessen an awesome amount of the mutilated sign highlights without losing its unique property, less memory space and figuring time are needed. Different transient occasions tried, for example, transitory interference, capacitor exchanging, voltage droop/swell, consonant bending, and flash demonstrate that the classifier can identify and group distinctive force unsettling influence sorts productively.

Xian-Xiang Li, Qian-Jin Zhang and Hong-Jun Xiao [13], present another way to deal with brushless DC engine which is in light of counterfeit neural system (ANN) and wavelet change. The methodology is composed taking into account a three-layer forward backward neural system, which prepares the system parameters in-line utilizing a slope descending error algorithm. The working and issue conditions of brushless DC machine are distinguished, in which the time-recurrence qualities of discrete wavelet change is utilized. The reenactment result demonstrates that the framework utilizing the methodology has great dynamic and static exhibitions, it is sensitive to fault and it has an unlimited applying prospect.

1.3 Different Types of Faults in an Induction Motor

Major faults in Induction machine are:

1. Bearing and insulation related faults-42%
2. Stator winding related faults-38%
3. Rotor related faults-10%
4. Other faults-10%

Among these bearing and insulation related faults are most common. Bearing faults cause some observable changes. The common indicators are increased temperature and high vibrations or noise level of machine. These faults are detected by analyzing readings of the spectrum of stator current and vibrations of the machine. However, vibration based detection methods require very high sensitive and precise vibration sensors and also direct access to the machine is required. Whereas, current monitoring is an easy approach to detect these faults as simple and cheap current sensors can be used.

Utilizing neural system we can take care of numerous issues without discovering and depicting technique for such critical thinking, without building calculations, even with no instance of individual information about the way of tackled issue. Just we have to have a few cases of comparable undertakings with arrangements. In the event that we have gathering of such illustrations we can utilize neural system, which first can take in these aftereffects of tackled issue (called preparing) and next can tackle numerous another comparative issues. It is truly a proficient method for critical thinking.

Second focal point is that now numerous equipment answers for neural systems are accessible. Various electronic and optoelectronic frameworks was produced on the base of neural systems structures, which are chipping away at the base of neural routines for data preparing. For this situation real playing point can monstrous parallel preparing which is conceivable in such equipment neural system. Indeed in natural mind all neurons are working at the same time. For vision, listening to and muscle control are actuated in the same time billons of organic neural cells. For counterfeit neural systems the same methodology can be abused too – yet just if there should be an occurrence of equipment arrangement.

1.4 Motivation

Maintenance of induction motors is one of the serious problems faced by most of the industries. According to Electric Power Research Institute motor reliable study [14], stator faults are responsible for 37% of the induction motor failures. According to Neale [16], the purchasing and installation costs of the equipments usually cost less than half of the total expenditure over the life of the machine for maintenance. According to Wowk [15], maintenance expenditure typically presents 15 to 40% of the total cost and it can be up to 80% of the total cost.

Having checked on the vast majority of the strategies for flaw judgment of an induction machine it is seen that precise models of the flawed machine and model based methods are basically needed for attaining to a decent fault diagnosis. Now and then it gets to be hard to acquire precise models of the defective machine furthermore in applying model based procedures. Then again, delicate figuring methodologies, for example, neural systems and wavelet methods give great investigation of a framework even of exact models are inaccessible. This proposition utilizes the Soft Computing strategies, for example, Back Propagation Algorithm (BPA) and Radial Basis Function Neural Network (RBFNN) to the recognition and area of a inter turn short circuit fault in the stator winding of an induction engine. Along these lines, a discrete wavelet system is utilized for the location of the seriousness of a inter turn short circuit fault in the stator winding of the induction machine.

3.6 Objectives of the Thesis

- 1 To measure the stator line voltages and current of an induction machine after applying varying voltages at no load condition from a three phase variac in healthy condition of the motor.
- 2 Then to emulate faulty condition in the motor by short circuiting the stator turns at the tappings taken out and then again measure the stator line voltages and current of the induction machine under faulty condition.
- 3 To apply different soft computing techniques such as BPA and RBFNN for the detection of the health condition
- 4 To propose discrete wavelets transform approach to detect the severity of stator inter-turn short circuit fault in the stator winding of the induction motor.

1.6 Organization of the Thesis

The thesis is partitioned in six sections. Other than this initial chapter, the accompanying chapters are exhibited.

Chapter–2 illustrates an experimental set up for the measurement induction motor stator phase current, line voltage and rotor speed both under healthy and stator inter-turn short circuit faulty condition. These induction motor readings are used to predict the healthiness of insulation of induction motor under faulty condition.

Chapter–3 deals with different neural network techniques such as BPA and RBFNN for the diagnosis of stator inter-turn short circuit fault of an induction motor. It explains each technique clearly using flow chart and training methodology used. It describes the commonly used radial basis functions and the typical RBF used in this thesis for the determination of the healthy condition of the induction motor insulation.

Chapter–4 In this chapter, application of different techniques of neural networks (NNs) are chosen such as back propagation algorithm (BPA) and radial basis function neural network (RBFNN) for inter-turn short circuit fault diagnosis in the stator winding of an induction motor. Different kinds of inputs are used to the neural networks such as stator line current, line voltage and rotor speed and the obtained output is compared with the desired healthiness of insulation condition and the difference between this two values is expressed in terms of root mean square error and the epoch no vs. root mean square error is also plotted for different values of learning and momentum rate. And lastly the above two techniques are compared.

Chapter–5 In this chapter, the discrete wavelet transform is implemented to diagnose the stator inter-turn short circuit fault of an induction motor. The stator line voltages and current are used as input data for the analysis of stator insulation condition under both healthy and faulty condition. By using the discrete wavelet transform, the approximation and detailed coefficients corresponding to the insulation condition of the motor are obtained. From these coefficients the severity of the fault condition can be determined.

Chapter–6 concludes the thesis and gives some suggestions for future work.

Chapter 2

Experimental Setup and Data Generation for Induction Motor Fault Diagnosis

2.1 Experimental Setup

A three phase induction motor with the ratings(as shown in table I) was connected to a 3 phase variac (Fig 2.1).The machine rewinding had been done from machine shop so that tapings were taken out from every $(N/7)^{\text{th}}$ part of stator winding.

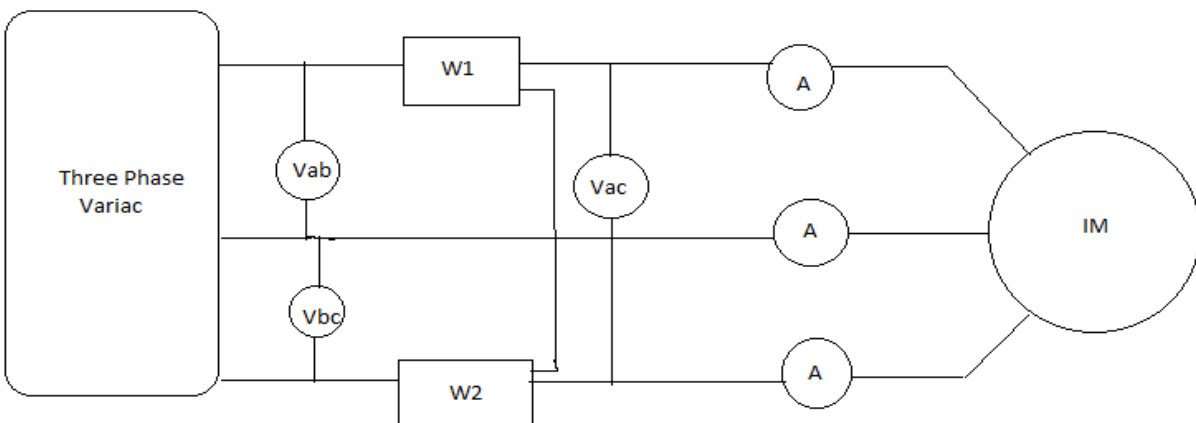


Fig.2.1 Block diagram of experimental setup

Table I: Induction motor ratings

Power	2 hp
Voltage	220/400 V
Current	13.63/3.75 A
Speed	1410 rpm
Number of poles	4
Total no. of turns	1656

2.2 Data generation through experiment

First under healthy condition voltage being applied to each phase was gradually increased from 40-115 V at no load and the three phase currents in the ammeters were noted. As well as the 3 line voltages and rotor speed in rpm was recorded with the help of a tachometer.

Secondly, machine was tried to emulate inter turn short circuit fault in stator winding

- Firstly turns between 1 to $(N/7)$ were shorted(Fig.2)
- Secondly turns between 1 to $(2N/7)$ were shorted
- Thirdly turns between $(N/7)$ to $(2N/7)$ were shorted
- Finally turns between 1 to $(3N/7)$ were shorted(Fig.3)

Each time the 3 phase currents, line voltages and rotor speed was measured.

The normalized values of current and voltage of phase R is taken as input data for the back propagation algorithm. By choosing appropriate values of learning and momentum rate parameter and through adjustment of weights in the BPA the healthiness of the machine is obtained.



Fig.2.2 Experimental Setup of a 3 phase 2 hp Induction Motor connected to variac at no load



Fig.2.3 Stator Winding Turn 1 to (N/7) Shorted



Fig.2.4 Stator Winding Turn 1 to (3N/7) Shorted

The machine rewinding had been done from machine shop so that tapings were taken out from every (N/7)th part of stator winding.

First under healthy condition voltage being applied to each phase was gradually increased from 40-115 V at no load and the 3 phase currents in the ammeters were noted. As well as the 3 line voltages and rotor speed in rpm was recorded with the help of a tachometer.

Secondly, machine was tried to emulate inter turn short circuit fault in stator winding

- Firstly turns between 1 to (N/7) were shorted(Fig.4)
- Secondly turns between 1 to (2N/7) were shorted
- Thirdly turns between (N/7) to (2N/7) were shorted
- Finally turns between 1 to (3N/7) were shorted(Fig.5)

Each time the 3 phase currents, line voltages and rotor speed was measured. The normalized values of current and voltage of phase R is taken as input data for the back propagation algorithm. By choosing appropriate values of learning and momentum rate parameter and through adjustment of weights in the BPA and RBFNN the healthiness of the machine is obtained. So back propagation algorithm and radial basis function neural network has been used to access the level of healthiness of the machine and root mean square error (RMS) is computed and plotted for each epoch. Then comparison is done between back propagation algorithm and radial basis function neural network. Values ranging from 0.1 to 0.9 decide the level of healthiness of the machine.

RMS error is calculated by the formula: $\sqrt{(e_1^2 + e_2^2 + e_3^2 + e_4^2 + \dots + e_M^2) / M}$

where e_i is the error calculated at the i th iteration

M is the total no of iterations

Table II: Induction motor readings under healthy condition

Sl No.	Current (A)			Voltage(V)			Speed(rpm)
	Phase R	Phase Y	Phase B	V_{RY}	V_{YB}	V_{BY}	
1	1.08	1.14	1.16	40.2	41.6	39.9	62
2	0.5	0.6	0.62	45.2	46.4	44.7	1330
3	0.4	0.48	0.5	51.6	52.8	50.7	1400
4	0.3	0.41	0.42	59.9	61	58.5	1434
5	0.3	0.4	0.41	66	67	64.9	1448
6	0.3	0.4	0.41	71.9	72.9	70.5	1458
7	0.3	0.4	0.4	75.3	76.8	74.2	1462
8	0.3	0.4	0.4	82	83.3	80.7	1468
9	0.3	0.4	0.4	90.8	92	89.8	1472
10	0.3	0.4	0.4	96	97	95	1474
11	0.29	0.4	0.4	104.1	104.6	102.3	1478
12	0.29	0.4	0.4	113.1	113.7	111.4	1496

Table III: Induction motor readings under faulty condition

Sl No.	No of turns shorted	Current (A)			Voltage(V)			Speed (rpm)
		Phase R	Phase Y	Phase B	V _{RY}	V _{YB}	V _{BY}	
1	1to(N/7)	0.68	0.5	0.6	49	51	50	1406
2		0.68	0.48	0.51	58	60	59	1418
3		0.71	0.5	0.51	70	72	72.9	1458
4		0.78	0.5	0.51	81.8	84	83.3	1468
5	1to(2N/7)	0.74	0.7	0.72	27.7	29.4	27.9	0
6		1.14	1.08	1.1	36.4	38.8	37.6	0
7		1.38	1.31	1.32	32.2	44.1	42.3	0
8		1.52	1.44	1.46	45	47.5	46	0
9	(N/7)to(2N/7)	1.18	1.18	1.2	39.4	40.6	41.6	0
10		1.24	1.18	1.35	43.9	46.1	44.6	0
11		1.4	1.45	1.52	48	50.7	49	0
12		0.4	0.45	0.49	53.5	55.9	54.4	1416
13	1to(3N/7)	0.5	0.46	0.49	21	22.9	22	0
14		0.63	0.6	0.62	24.9	27	25.1	0
15		0.92	0.88	0.89	31.4	33.7	32	0
16		1.14	1.07	1.08	36.5	38.7	37.2	0

2.3 Assumptions made

Value \geq 0.8 indicates very healthy condition means no fault has occurred

0.6 \leq Value $<$ 0.8 indicates incipient fault has start occurring

Value $<$ 0.6 indicates major fault

Formula used for normalization of data: $X_i = (X_i - X_{min}) / (X_{max} - X_{min})$

Where X_i is the ith data

X_{min} is the minimum value of X among the set of given data

X_{max} is the maximum value of X among the set of given data

Table IV: Normalized Data of R phase

SI No.	Current	Voltage	Healthiness of Insulation	Healthiness of Bearing
1	0.6423	0.208	0.9	0.9
2	0.171	0.263	0.9	0.9
3	0.0894	0.33	0.9	0.9
4	0.00813	0.4224	0.9	0.9
5	0.00813	0.4886	0.9	0.9
6	0.00813	0.553	0.9	0.9
7	0.00813	0.59	0.9	0.9
8	0.00813	0.66	0.9	0.9
9	0.00813	0.758	0.9	0.9
10	0.00813	0.814	0.9	0.9
11	0	0.9023	0.9	0.9
12	0	1	0.9	0.9
13	0.3171	0.304	0.65	0.9
14	0.3171	0.4017	0.6	0.9
15	0.3415	0.532	0.57	0.9
16	0.3984	0.66	0.55	0.9
17	0.3695	0.0727	0.5	0.9
18	0.6911	0.1672	0.35	0.9
19	0.8862	0.1216	0.15	0.9
20	1	0.261	0.1	0.9
21	0.7236	.1998	0.3	0.9
22	0.77	.249	0.25	0.9
23	0.9	.293	0.12	0.9
24	0.0894	.353	0.6	0.9
25	0.171	0	0.4	0.9
26	0.2764	0.0423	0.37	0.9
27	0.512	.1129	0.3	0.9
28	0.6911	.9597	0.1	0.9

2.4 Chapter Summary

This chapter presents an experimental setup for the measurement of induction motor parameters such as stator current, stator line voltages and rotor speed both under healthy and stator inter-turn short circuit fault conditions. For these measurements we have applied variac voltage varied in steps from 40-115 V under both healthy and shorting the stator winding for every two turns sequentially, beginning with turn '1' and ending with turn 710 of the induction motor.

Chapter 3

Different Artificial Neural Network Techniques

3.1 Introduction

In this chapter, application of different techniques of neural networks (NNs) are chosen such as Back Propagation Algorithm (BPA) and Radial Basis Function Neural Network (RBFNN) for inter-turn short circuit fault diagnosis in the stator winding of an induction motor. Different kinds of inputs are used to the neural networks such as current, voltage and speed for the induction motor stator fault diagnosis. It is seen that when the motor is faulty then there is change in values of stator line voltages, current and the rotor speed so these parameters are used to diagnose the faulty condition. The normalized values of current and voltages of one phase are taken to be as input data while taking the healthiness of insulation as the targeted data.

3.2 Chapter Objectives

- 1 To study the various soft computing techniques suitable for the fault diagnosis of a three phase squirrel cage induction motor.
- 2 To employ BPA for training MLPNN.
- 3 Designing RBFNN in view of improving the training performance.

3.3 Multilayer Perceptron Neural Network

In this section, neural systems have been used to diagnose the stator inter turn short circuit fault. Neural systems have picked up notoriety over different methods because of their speculation capacity, which implies that they find themselves able to perform palatably even for unseen faults. Neural systems can perform fault diagnosis without the need of perplexing and thorough scientific models. Furthermore, heuristic translation of machine conditions which at times just people are

equipped for doing can be effortlessly actualized in the neural systems through directed learning. For some deficiency identification plans excess data is accessible and can be utilized to attain more exact results. This idea can be effortlessly actualized in neural system employing its numerous input parallel handling highlights to upgrade the strength of the system execution.

3.3.1 Back Propagation Algorithm (BPA)

A set of training data is given to the system. The system processes its output pattern, and if there is an error - the weights are modified to lessen this error. In a back-propagation neural system, the learning calculation has two stages. To begin with, a preparation data example is introduced to the system input layer. The system proliferates the data design from layer to layer until the output example is created by the output layer. On the off chance that this example is not quite the same as the sought output, an error is computed and afterward proliferated in reverse through the system from the output layer to the input layer. The weights are changed as the error is propagated. Learning rate is a consistent in the calculation of neural system that influences the velocity of learning. The higher the rate is set, the faster the network will learn, but if there is large variability in the input the network will not learn very well. Most standard back propagation algorithms employ a momentum term in order to speed up the convergence while avoiding network instability, with weight values oscillating erratically as they converge to a solution.

The training of BPA involves the following steps:

$s1 = \text{input} * w_a$	$w_a =$ weight vector between input and hidden layer
$a1 = 1 / (1 + \exp(-s1))$	$a1 =$ first activation function
$s2 = a1 * w_b$	$w_b =$ weight vector between hidden and output layer
$a2 = 1 / (1 + \exp(-s2))$	$a2 =$ second activation function
$\text{erro} = \text{target_data} - a2$	$\text{erro} =$ error at output layer
$\text{err} = \text{erro} * a2^{-1} * (1 - a2)$	
$\text{errh} = \text{err} * w_b^{-1} * a1^{-1} * (1 - a1)$	$\text{errh} =$ error at hidden layer

$$dw_b = l * a_1^{-1} * err + m * dw_b \quad dw_b = \text{modification of weight vector } w_b$$

$$dw_a = l * input^{-1} * err_h + m * dw_a \quad dw_a = \text{modification of weight vector } w_a$$

$$w_a = w_a + dw_a \quad \text{update of weight vector } w_a$$

$$w_b = w_b + dw_b \quad \text{update of weight vector } w_b$$

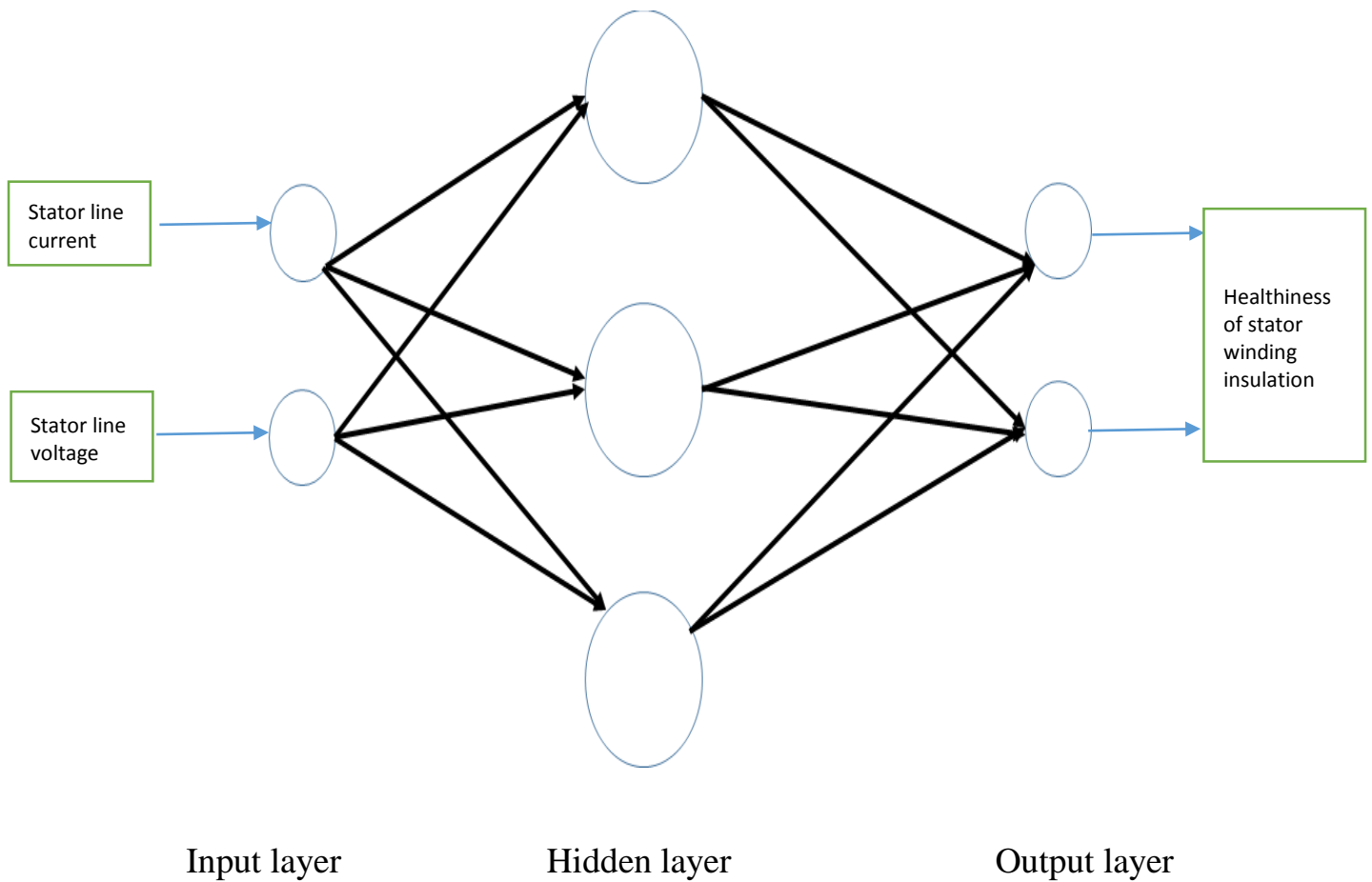
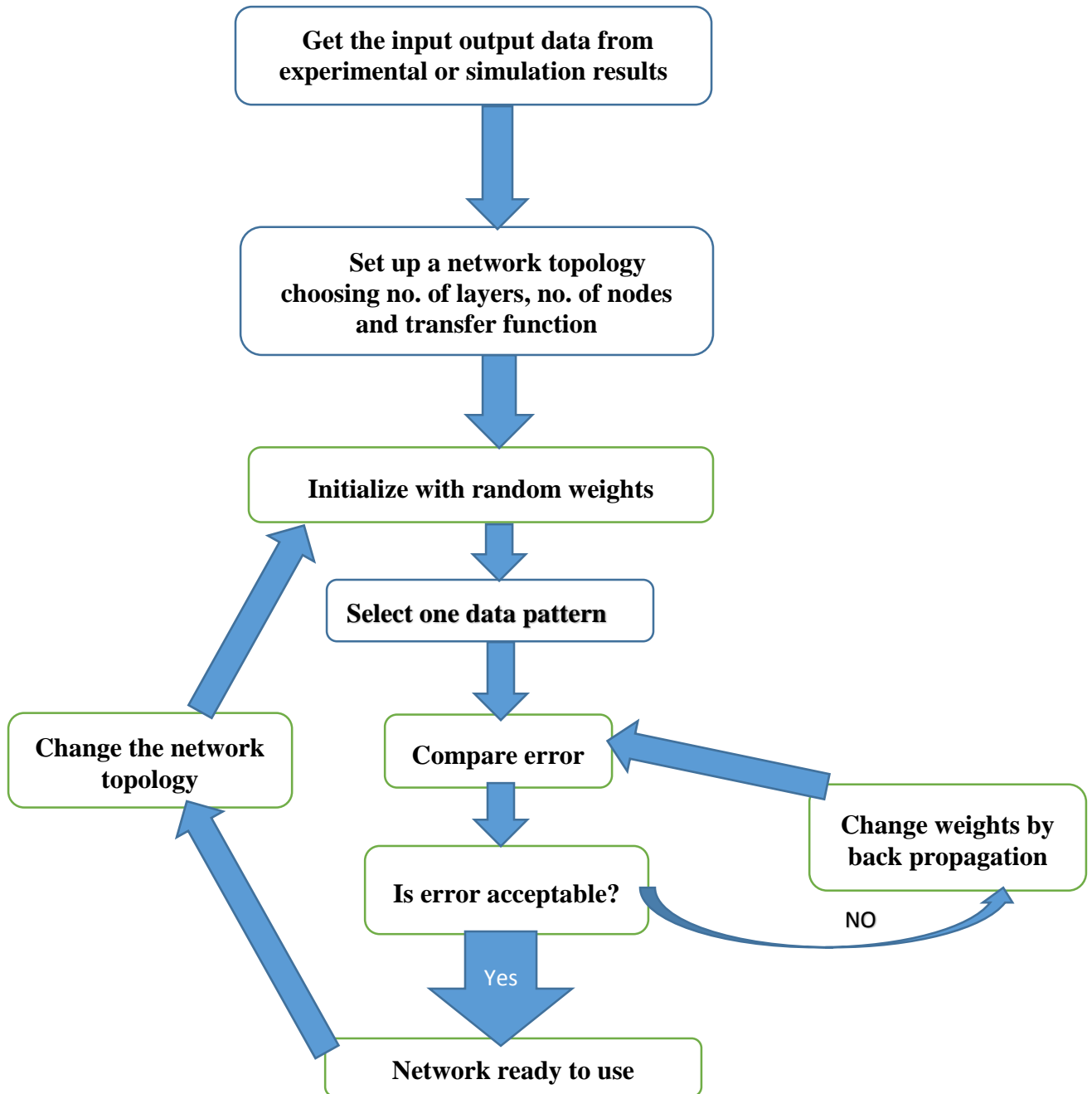


Fig 3.1 Configuration of Multilayer Perceptron Neural Network (MLPNN)

3.3.2 Flow chart for Back Propagation Algorithm



3.4 Radial Basis Function Neural Network

Radial Bases Functions Networks (RBFN) was firstly proposed by Broomhead and Lowe in 1988. The thought of Radial Basis Function (RBF) Networks gets from the hypothesis of capacity close estimation. We have as of now perceived how BPA with hidden layer of sigmoidal units can figure out how to approximate functions. RBF Networks take a somewhat diverse methodology. Their primary highlights are:

1. They are two-layer feed forward systems.
2. The hidden nodes implement a set of radial basis functions (e.g. Gaussian functions).
3. The output nodes actualize straight summation works as in a BPA.
4. The system training is separated into two stages: first the weights from the input to hidden layer are set, and afterward the weights from the hidden up to outer layer.
5. The preparation/learning is quick.
6. The systems are great at introduction.

3.4.1 Commonly used Radial Basis Functions

A scope of hypothetical and experimental studies have shown that numerous properties of the interpolating function are insensitive to the precise form of the basis functions $f(r)$. Some of the most commonly used basis functions are:

1. Linear Functions:

$$\phi(r) = r$$

2. Cubic Functions:

$$\phi(r) = r^3$$

3. Gaussian Functions:

$$\phi(r) = \exp(-r^2 / (2\sigma^2))$$

4. Multi-Quadratic Functions:

$$\phi(r) = (r^2 + \sigma^2)^{1/2}$$

5. Generalized Multi-Quadratic Functions:

$$\phi(r) = (r^2 + \sigma^2)^\beta \quad 0 < \beta < 1$$

6. Inverse Multi-Quadratic Function:

$$\phi(r) = (r^2 + \sigma^2)^{-1/2}$$

7. Thin Plate Spline Function:

$$\phi(r) = r^2 \ln(r)$$

8. Shifted Logarithm:

$$\phi(r) = \log(r^2 + \sigma^2)$$

9. Generalized Inverse Multi-Quadratic:

$$\phi(r) = (r^2 + \sigma^2)^{-\alpha} \quad \alpha > 0$$

where $r = \|x - c\|^2$. The Gaussian and Inverse Multi-Quadratic Functions are localized in the sense that $\phi(r)$ tends to 0 as $\|r\|$ tends to infinity. For all the other mentioned functions: $\phi(r)$ tends to infinity as $\|r\|$ tends to infinity.

3.4.2 Typical Radial Basis Function that has been used for the simulation

Radial basis function (RBF) networks typically have three layers: an input layer, a hidden layer with a RBF activation function and an output layer. The input can be modeled as a vector of real numbers. The output of the network is then a scalar function of the input vector and is given by

$$\Phi(\mathbf{x}) = \sum a_i \rho(\|\mathbf{x} - \mathbf{c}_i\|)$$

This summation is done from $i=1$ to N

where N is the quantity of neurons in the concealed layer, \mathbf{c}_i is the middle vector for neuron i and a_i is the heaviness of neuron i in the linear output neuron. Functions that depend just on the separation from a middle vector are radially symmetric about that vector, thus the name RBF. In the fundamental shape all inputs are joined with every hidden neuron.

The norm is typically taken to be the Euclidean distance and the radial basis function is commonly taken to be Gaussian function

$$\rho(\|\mathbf{x} - \mathbf{c}_i\|) = \exp[-\beta \|\mathbf{x} - \mathbf{c}_i\|^2]$$

where $\beta=1/(\sigma^2)$, $\sigma=d_{\max}/\sqrt{m}$

D_{\max} =maximum distance between 2 centers and m =no of centers

The Gaussian basis functions are local to the center vector in the sense that

$$\lim_{\|\mathbf{x}\| \rightarrow \infty} \rho(\|\mathbf{x} - \mathbf{c}_i\|) = 0$$

i.e. changing parameters of one neuron has just a little impact for info values that are far from the focal point of that neuron. Given certain mellow conditions on the state of the actuation capacity, RBF systems are widespread approximators on a conservative subset of R^n . This implies that a RBF system with enough concealed neurons can estimated any persistent capacity with discretionary accuracy. The parameters a_i , c_i and β_i are resolved in a way that enhances the fit in the middle of ϕ and the information.

Notwithstanding the above unnormalized structural planning, RBF systems can be standardize.

In this case the mapping is

$$\phi(\mathbf{x}) = \sum \mathbf{a}_i \rho(\|\mathbf{x} - \mathbf{c}_i\|) / \sum \rho(\|\mathbf{x} - \mathbf{c}_i\|) = \sum \mathbf{a}_i \mathbf{u}(\|\mathbf{x} - \mathbf{c}_i\|)$$

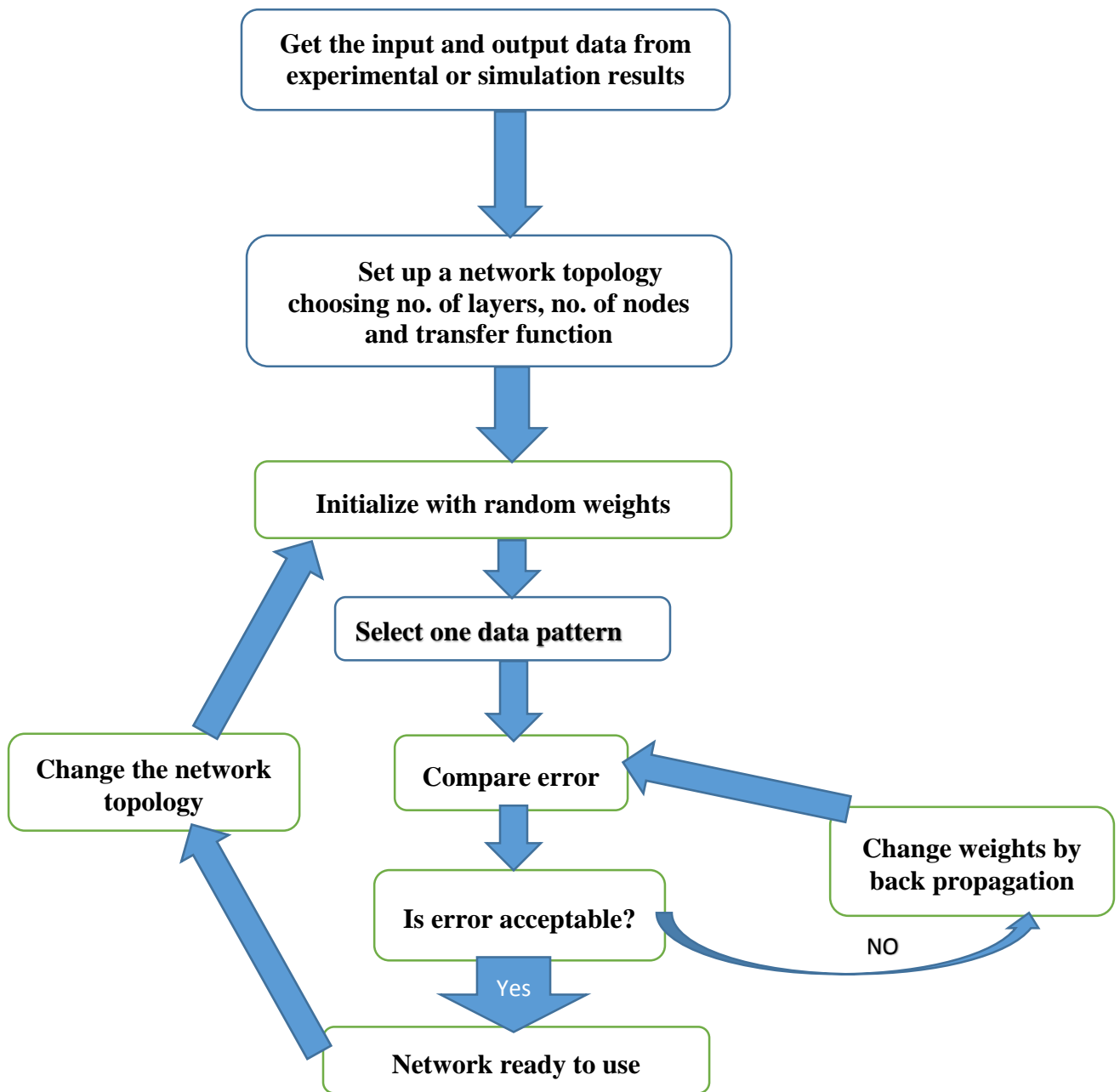
where each summation is done from $i=1$ to N and

$$\mathbf{u}(\|\mathbf{x} - \mathbf{c}_i\|) = \rho(\|\mathbf{x} - \mathbf{c}_i\|) / \sum \rho(\|\mathbf{x} - \mathbf{c}_j\|)$$

where each summation is done from $j=1$ to N .

This is known as a “normalized radial basis function”.

3.4.3 Flow chart for Radial Basis Function Neural Network



3.5 Training Methodology of the Neural Networks

Training of the neural network is the process of adjusting the weights. Firstly, the network outputs and the difference between the actual output and the targeted output is calculated for the initialized weights and the biases in all the neurons are adjusted to minimize the error by back propagation of the error backwards. The network outputs and the error are calculated again with the modified weights and the process is repeated at each epoch until a satisfied output is obtained and the error is appreciably small.

3.6 Chapter Summary

This chapter deals with different neural network techniques such as BPA and RBFNN for the diagnosis of stator inter-turn short circuit fault of an induction motor. It explains each technique clearly using flow chart and training methodology used. It describes the commonly used radial basis functions and the typical RBF used in this thesis for the determination of the healthy condition of the induction motor insulation.

Chapter 4

Data Generation from the Simulated Neural Networks

4.1 Introduction

For the purpose of simulation firstly the momentum rate (m) is varied at a fixed learning rate (l) and the most appropriate rates are chosen and then at those momentum rates learning rates are varied and finally the appropriate learning rate is chosen which gives least mean square error for back propagation algorithm. Then in order to improve the training performance radial basis function neural network is designed and the minimum root mean square error i.e. the difference between the target data i.e. the condition of insulation under healthy condition (taking it to be 0.9) and the obtained condition of insulation for different values of m and l is obtained.

4.2 Simulation Set-up

The network with 2 nodes in the input, 4 nodes in hidden and 2 nodes in output layer is designed. Firstly, the network outputs and the difference between the actual output and the targeted output is calculated from the initialized weights and the biases in all the neurons are adjusted to minimize the error by back propagation of the error layer by layer. The network outputs and the error are calculated again with the modified weights and the process is repeated at each epoch until a satisfied output is obtained and the error is appreciably small.

4.3 Results of Simulation of Back Propagation Algorithm

In a BPA first, a input pattern is presented to the network input layer. The network propagates the input pattern from layer to layer until the output pattern is generated by the output layer. If this

pattern is different from the desired output, an error is calculated and then propagated backwards through the network from the output layer to the input layer. The weights are modified as the error is propagated. Thus the results of the trained network are presented in the following tables.

Table V: Desired healthiness of insulation for $l=0.1$, $m=0.4$ and $m=0.5$

SI No.	Desired Healthiness of Insulation	Obtained Healthiness of Insulation at $m=0.4$	Obtained Healthiness of Insulation at $m=0.5$
1	0.9	0.5817	0.5755
2	0.9	0.7854	0.7829
3	0.9	0.8287	0.8264
4	0.9	0.8666	0.8645
5	0.9	0.8686	0.8667
6	0.9	0.8704	0.8688
7	0.9	0.8715	0.87
8	0.9	0.8733	0.872
9	0.9	0.8758	0.8747
10	0.9	0.8772	0.8763
11	0.9	0.8820	0.8814
12	0.9	0.8841	0.8838
13	0.65	0.7154	0.7128
14	0.6	0.7199	0.717
15	0.57	0.7138	0.7104
16	0.55	0.6929	0.6884
17	0.5	0.6815	0.6789
18	0.35	0.5733	0.5681
19	0.15	0.5380	0.5333
20	0.1	0.5267	0.5217
21	0.3	0.5668	0.5613
22	0.25	0.5587	0.5527
23	0.12	0.5387	0.5327
24	0.6	0.8319	0.8301
25	0.4	0.7790	0.7772
26	0.37	0.7246	0.7224
27	0.3	0.6214	0.6170
28	0.1	0.5971	0.5850

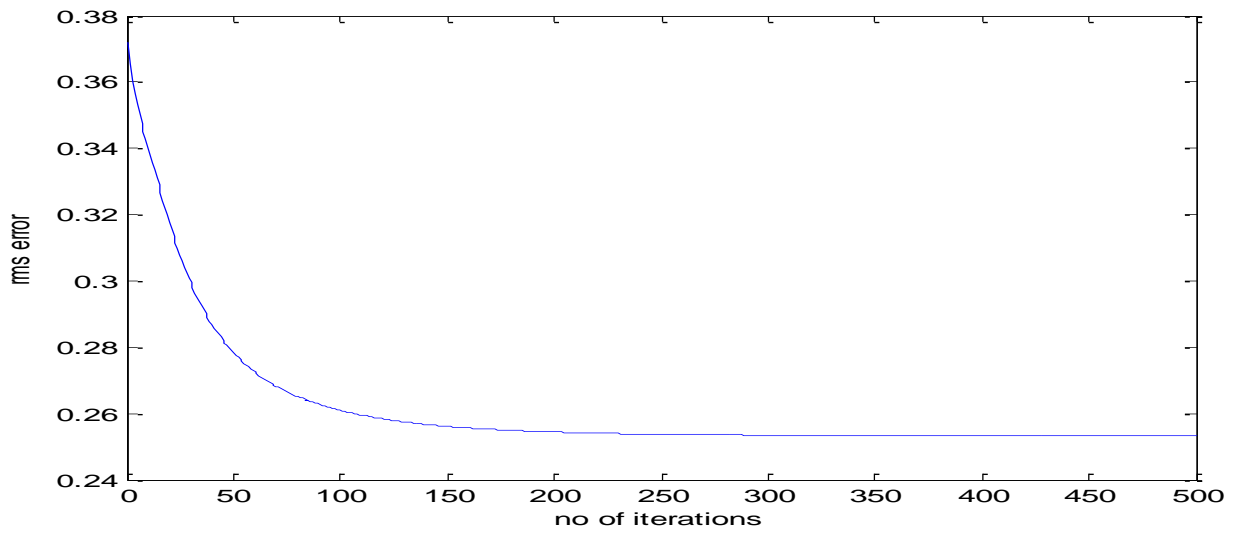


Fig4.1 Root mean square error in the healthiness of insulation condition for $l=0.1$, $m=0.4$ using BPA

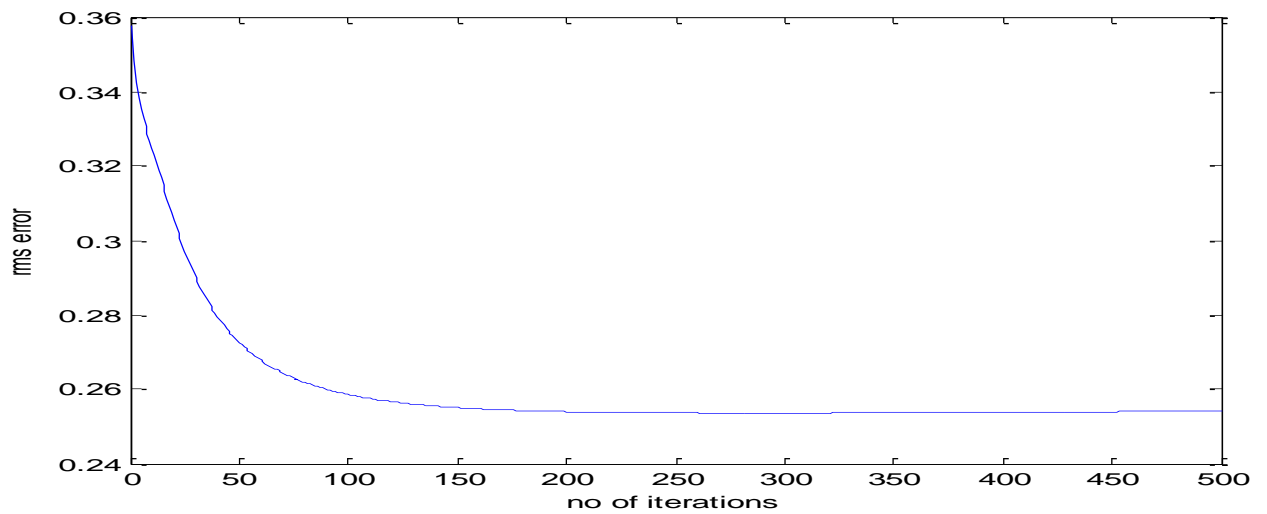


Fig4.2 Root mean square error in the healthiness of insulation condition for $l=0.1$, $m=0.5$ using BPA

Table VI: Desired healthiness of insulation for $m=0.5$, $l=0.2$ and $l=0.3$

Sl No.	Desired Healthiness of Insulation	Obtained Healthiness of Insulation at $l=0.2$	Obtained Healthiness of Insulation at $l=0.3$
1	0.9	0.511	0.5271
2	0.9	0.7447	0.7618
3	0.9	0.7931	0.819
4	0.9	0.8365	0.868
5	0.9	0.8398	0.8697
6	0.9	0.8431	0.8712
7	0.9	0.8454	0.8722
8	0.9	0.8491	0.8736
9	0.9	0.8541	0.8753
10	0.9	0.8573	0.8764
11	0.9	0.8648	0.8817
12	0.9	0.8695	0.8833
13	0.65	0.6704	0.6764
14	0.6	0.6723	0.6775
15	0.57	0.6634	0.665
16	0.55	0.6378	0.6353
17	0.5	0.6481	0.651
18	0.35	0.5112	0.5322
19	0.15	0.4748	0.5062
20	0.1	0.4427	0.4904
21	0.3	0.4993	0.5243
22	0.25	0.4834	0.5141
23	0.12	0.4534	0.4956
24	0.6	0.8007	0.8266
25	0.4	0.7583	0.7747
26	0.37	0.6961	0.7014
27	0.3	0.5722	0.5763
28	0.1	0.506	0.5132

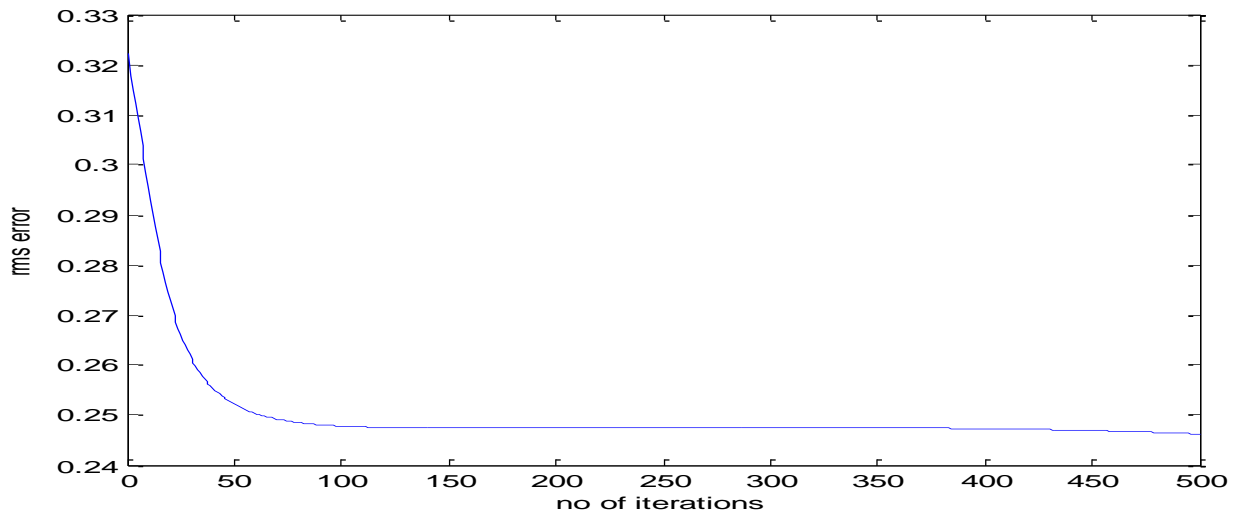


Fig 4.3 Root mean square error in the healthiness of insulation condition for $l=0.2$, $m=0.5$ using BPA

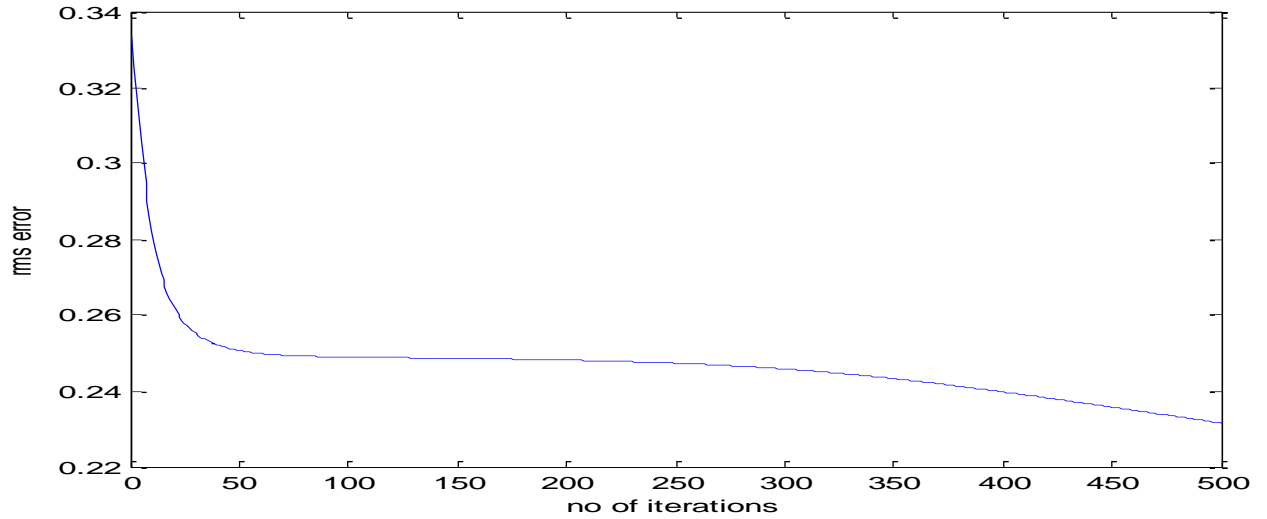


Fig 4.4 Root mean square error in the healthiness of insulation condition for $l=0.3$, $m=0.5$ using BPA

Table VII: Desired healthiness of insulation for $m=0.4$, $l=0.1$ and $l=0.2$

Sl No.	Desired Healthiness of insulation	Obtained Healthiness of insulation at $l=0.1$	Obtained Healthiness of insulation at $l=0.2$
1	0.9	0.5817	0.5679
2	0.9	0.7854	0.7806
3	0.9	0.8287	0.8298
4	0.9	0.8666	0.871
5	0.9	0.8686	0.8725
6	0.9	0.8704	0.8736
7	0.9	0.8715	0.8744
8	0.9	0.8733	0.8754
9	0.9	0.8758	0.8765
10	0.9	0.8772	0.8773
11	0.9	0.8820	0.8813
12	0.9	0.8841	0.882
13	0.65	0.7154	0.7111
14	0.6	0.7199	0.7157
15	0.57	0.7138	0.708
16	0.55	0.6929	0.6846
17	0.5	0.6815	0.6767
18	0.35	0.5733	0.572
19	0.15	0.5380	0.5416
20	0.1	0.5267	0.5359
21	0.3	0.5668	0.5657
22	0.25	0.5587	0.5596
23	0.12	0.5387	0.544
24	0.6	0.8319	0.8345
25	0.4	0.7790	0.7795
26	0.37	0.7246	0.7177
27	0.3	0.6214	0.609
28	0.1	0.5971	0.5802

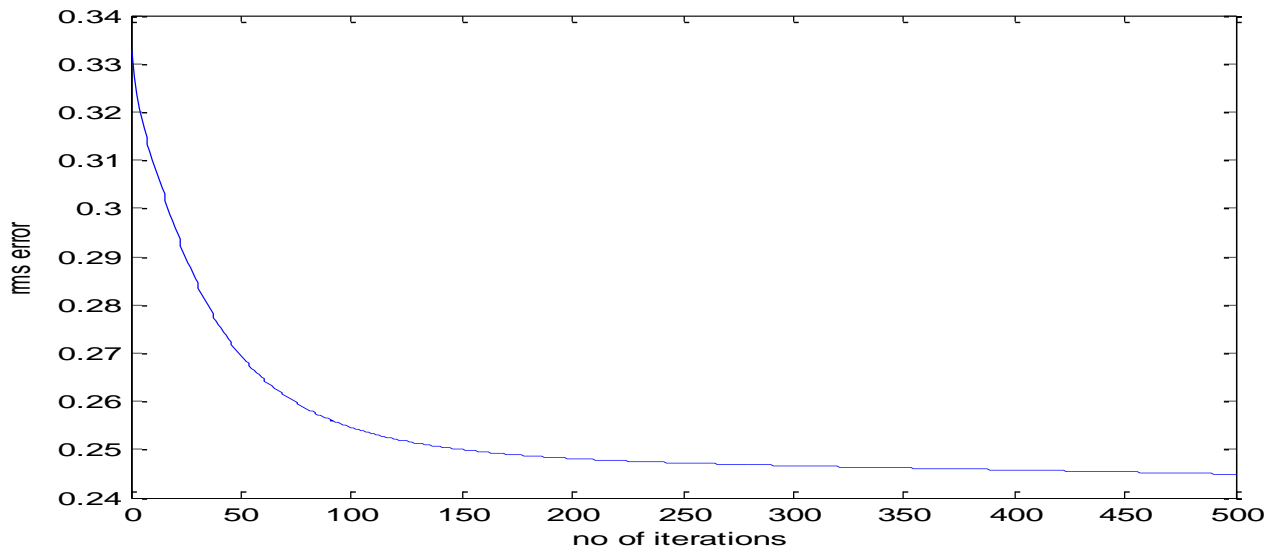


Fig 4.5 Root mean square error in the healthiness of insulation condition for $l=0.1$, $m=0.4$ using BPA

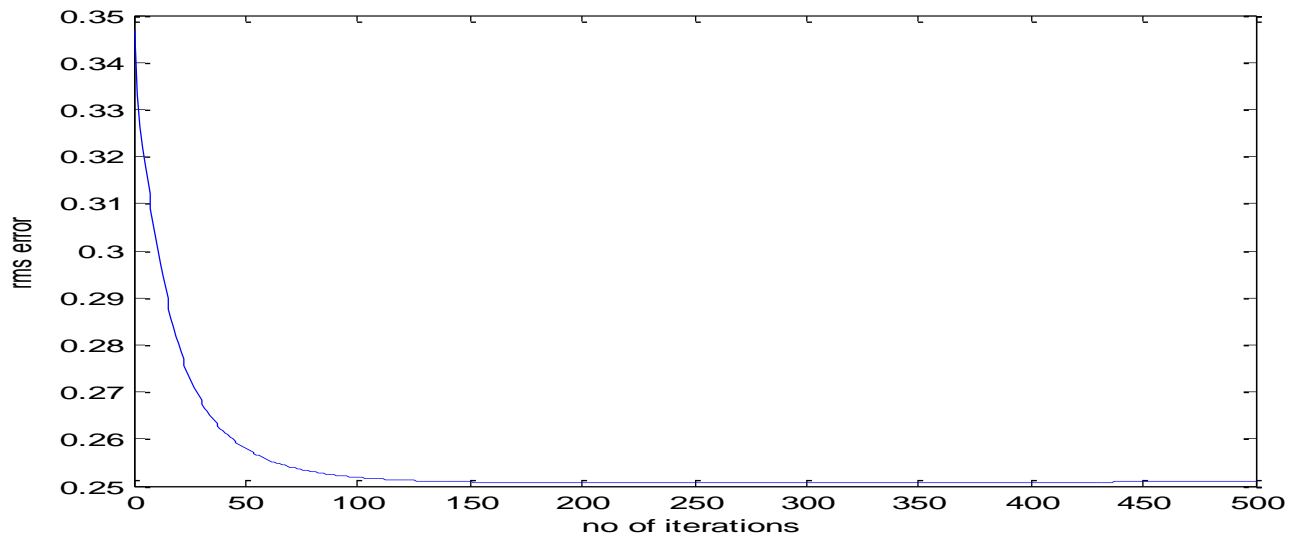


Fig 4.6 Root mean square error in the healthiness of insulation condition for $l=0.2$, $m=0.5$ using BPA

4.4 Results of Simulation of Radial Basis Function Neural Network

Table VIII: Desired healthiness of insulation for $l=0.1$, $m=0.4$ and $m=0.5$

SI No.	EPOCH No.	Approximate root mean square error at $m=0.4$	Approximate root mean square error at $m=0.5$
1	1	0.0139	0.0140
2	2	0.0136	0.0137
3	3	0.0133	0.0135
4	4	0.0128	0.0133
5	5	0.0119	0.0129
6	6	0.0112	0.0119
7	7	0.0110	0.0114
8	8	0.0121	0.0118
9	9	0.0124	0.0124
10	10	0.0120	0.0128
11	11	0.0119	0.0122
12	12	0.0121	0.0119
13	13	0	0.0118
14	14	0	0.0119
15	15	0	0.0121
16	16	0	0

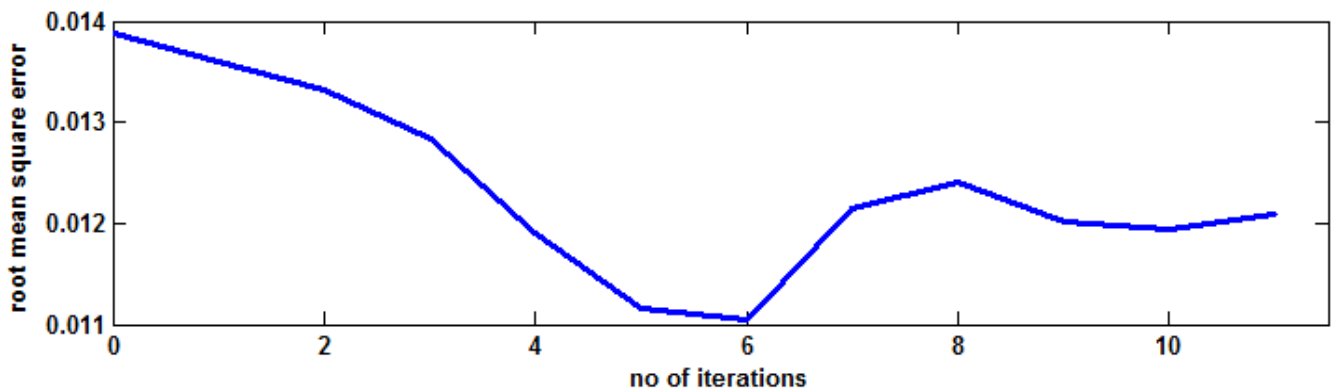


Fig 4.7 Root mean square error in the healthiness of insulation condition for $l=0.1$, $m=0.4$ using RBFNN

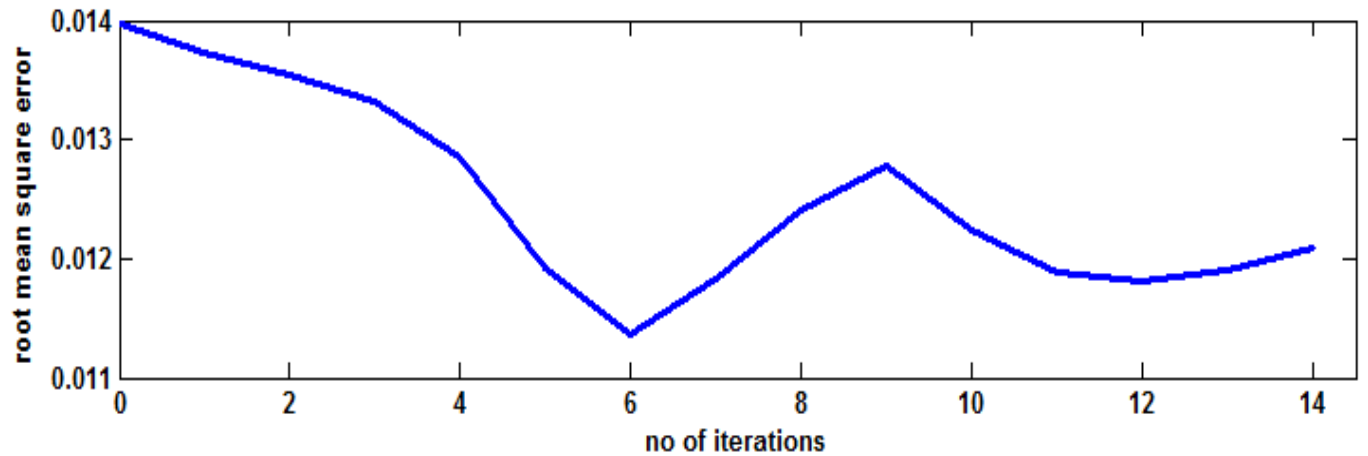


Fig 4.8 Root mean square error in the healthiness of insulation condition for $l=0.1$, $m=0.5$ using RBFNN

Table IX: Desired healthiness of insulation for $m=0.4$, $l=0.2$ and $l=0.3$

SI No.	EPOCH No.	Approximate root mean square error at $l=0.2$	Approximate root mean square error at $l=0.3$
1	1	0.0140	0.0141
2	2	0.0138	0.0139
3	3	0.0137	0.0137
4	4	0.0135	0.0136
5	5	0.0133	0.0133
6	6	0.0130	0.0127
7	7	0.0122	0.0119
8	8	0.0115	0.0114
9	9	0.0114	0.0114
10	10	0.0124	0.0119
11	11	0.0120	0.0122
12	12	0.0126	0
13	13	0.0138	0
14	14	0	0

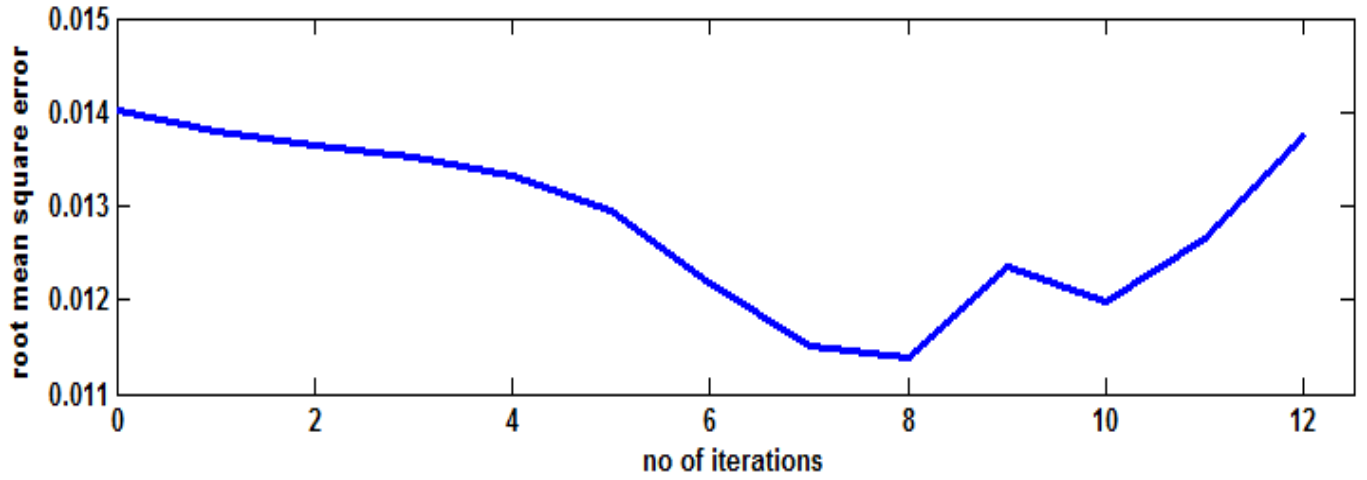


Fig 4.9 Root mean square error in the healthiness of insulation condition for $l=0.2$, $m=0.4$ using RBFNN

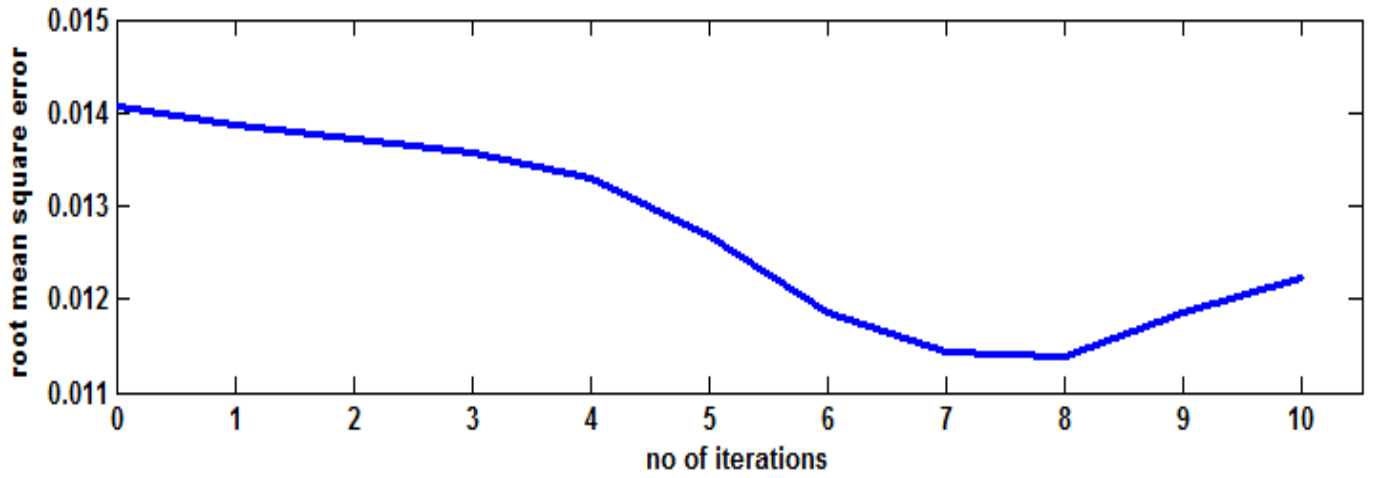


Fig 4.10 Root mean square error in the healthiness of insulation condition for $l=0.3$, $m=0.4$ using RBFNN

Table X: Desired healthiness of insulation for $m=0.5$, $l=0.2$ and $l=0.3$

SI No.	EPOCH No.	Approximate root mean square error at $l=0.1$	Approximate root mean square error at $l=0.2$
1	1	0.0140	0.0142
2	2	0.0138	0.0141
3	3	0.0137	0.0140
4	4	0.0135	0.0140
5	5	0.0133	0.0138
6	6	0.0127	0.0135
7	7	0.0118	0.0126
8	8	0.0117	0.0120
9	9	0	0.0122
10	10	0	0.0132
11	11	0	0

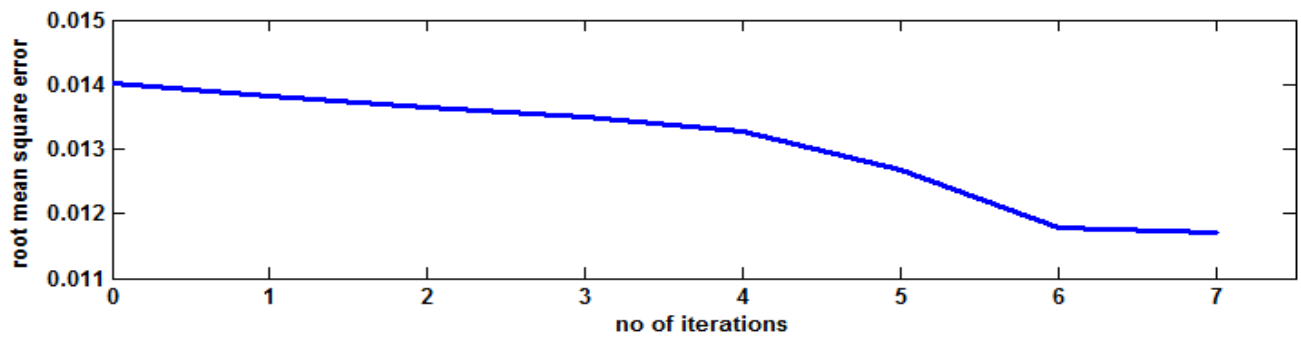


Fig 4.11 Root mean square error in the healthiness of insulation condition for $l=0.2$, $m=0.5$ using RBFNN

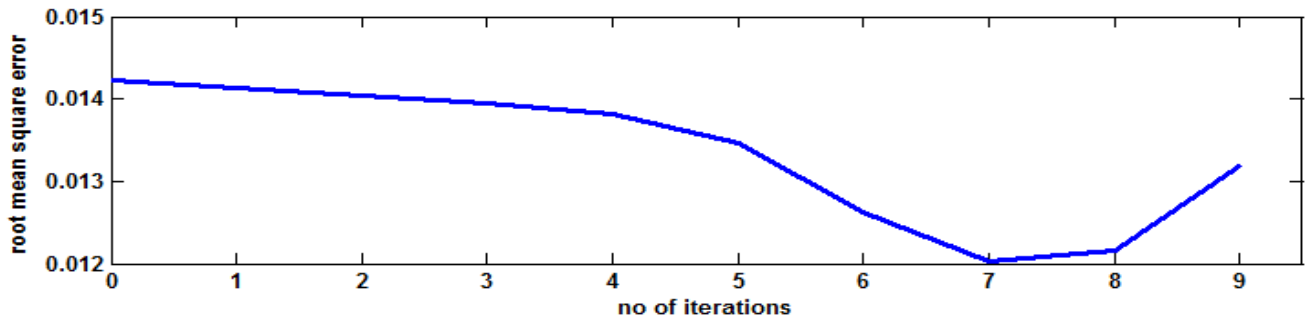


Fig 4.12 Root mean square error in the healthiness of insulation condition for $l=0.3$, $m=0.5$ using RBFNN

4.5 Comparison between RBFNN and BPA

After successfully training the both the multi-layer perceptron neural networks we find that radial basis function neural network gets trained much faster and the minimum root mean square (RMS) error obtained is around 0.013 which is much smaller than that obtained in case of back propagation algorithm which was 0.065, which is almost five times more than that in case of radial basis function neural network. RBFNN requires only a maximum of 25 EPOCH to get trained whereas BPA requires almost 500 EPOCH for getting properly trained.

Table XI: Difference between the RMS errors obtained for $l=0.2$ and $m=0.5$

EPOCH No.	BPA	RBFNN
1	0.1014	0.0142
2	0.0959	0.0141
3	0.0931	0.0140
4	0.0916	0.0140
5	0.0905	0.0138
6	0.0897	0.0135
7	0.0888	0.0126
8	0.0880	0.0120
9	0.0872	0.0122
10	0.0865	0.0132
11	0.0857	0
12	0.0850	0
13	0.0843	0
14	0.0836	0
15	0.0829	0

4.5 Chapter Summary

We see that Radial Basis Function Neural Network requires very little memory for approximation and also gets trained very fast with fewer number of training data examples. When for a given set of training data Back Propagation Algorithm requires 500 epoch Radial Basis Function Neural Network requires only 25 or less number of epoch as seen in figure 4.7, 4.8, 4.9, 4.10, 4.11 and 4.12. Also the root mean square in case of Radial Basis Function Neural Network is far less than in case of Back Propagation Algorithm so we can conclude that Radial Basis Function Neural Network is better approximation method and more efficient than Back Propagation Algorithm.

Chapter 5

Short Circuit Inter Turn Fault Diagnosis using Discrete Wavelet Transform

5.1 Introduction

In different genuine applications, for example, remote detecting and therapeutic picture determination, picture combination assumes basic part and it is more prominent for picture handling applications. In light of lacking nature of commonsense imaging frameworks the catch pictures or obtained pictures are ruined from different commotion consequently combination of picture is a coordinated methodology where diminishment of clamor and holding the first highlights of picture is fundamental. Picture combination is the methodology of extricating significant visual data from two or more pictures and consolidating them to frame one melded picture. Discrete Wavelet Transform (DWT) has an extensive variety of use in combination of clamor pictures.

Wavelet Transform (WT) is a powerful signal analysis tool that has been used successfully in many areas for more than a decade. It is the transform of a signal from one form to another form. It does not change the information content present in the signal. The multi-resolution analysis (MRA) is one of the most active branches of the wavelet transform (WT) theory. The multi resolution analysis (MRA) provides an effective way to examine the features of a signal at different frequency bands. This feature may be essential for pattern recognition. Hence it is well suited for the fault identification and classification problems in an induction motor.

5.2 Chapter Objectives

- In view of improving the training performance another technique is employed known as Discrete Wavelet Transform.
- The training set of data is presented to the network and are passed through high and low

pass filter for decomposition of the data using down sampling.

- The detailed and approximation coefficients are obtained from high and low pass filter respectively.
- Then the above coefficients are also obtained for the target and actual outputs.
- The difference between the coefficients of obtained and target outputs are computed and root mean square error is calculated and plotted.

5.3 Discrete Wavelet Transform

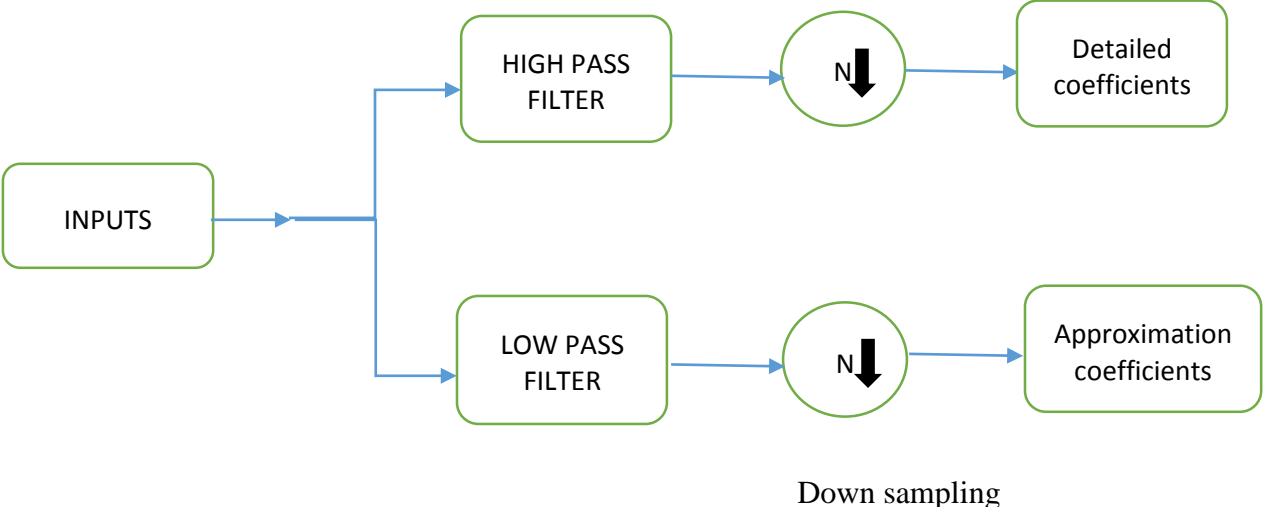
Discrete wavelet transform (DWT) calculations have gotten to be guidelines instruments for handling of signs and pictures in a few territories in exploration and industry. The primary DWT structures were in view of the minimalistically upheld conjugate quadrature channels (CQFs). However, a downside in CQFs is identified with the nonlinear stage impacts, for example, picture obscuring and spatial separations in multi-scale investigations. Actually, in biorthogonal discrete wavelet transform (BDWT) the scaling and wavelet channels are symmetric and straight stage. The BDWT calculations are normally developed by a step sort system called lifting plan. The system comprises of consecutive down and elevating steps and the remaking of the sign is made by running the lifting system in converse request. Proficient lifting BDWT structures have been created for VLSI and microchip applications. The investigation and union channels can be executed by number math utilizing just enlist shift s and summations. Numerous BDWT-based information and picture transforming instruments have outflanked the customary discrete cosine transform (DCT) -based methodologies.

As DWT gives both octave-scale recurrence and spatial timing of the examined sign, it is continually used to unravel and treat more propelled issues. One of the primary troubles in multi-scale investigation is the reliance of the aggregate vitality of the wavelet coefficients in diverse scales on the partial movement s of the broke down sign. In the event that we have a discrete sign $x[n]$ and the relating time moved sign $x[n-\tau]$, where $\tau \in [0, 1]$, there may exist a noteworthy distinction in the vitality of the wavelet coefficients as a component of the time shift. In movement invariant systems the genuine and fanciful parts of the intricate wavelet coefficients are more or less a Hilbert change pair. The vitality of the wavelet coefficients measures up to the envelope, which gives smoothness and estimated movement invariance. Utilizing two parallel DWT banks,

which are developed so that the motivation reactions of the scaling channels have half-specimen postponed forms of one another, the relating wavelets are a Hilbert change pair. The double tree CQF wavelet channels don't have coefficient symmetry and the nonlinearity meddles with the spatial timing in distinctive scales and avoids exact factual relationships. Hence the present advancements in principle and uses of wavelets are focused on the double tree BDWT structure.

5.4 Methodology adopted to implement DWT for Fault Diagnosis of Induction Motor

In order to train the wavelet neural network (WNN) 28 samples are taken and these 28 set of values of stator line voltages and current of induction motor taken under no load condition in healthy as well as faulty condition are down sampled by discrete wavelet transform algorithm. Then those down sampled values are given to the neural network and the detailed and approximation coefficients are obtained. All these detailed and approximation coefficients are trained through RBFNN individually. Detailed coefficients and approximation coefficients are obtained from high pass and low pass filter respectively when the samples are allowed to pass through it as shown in Fig 5.1.



Where N=2 which specify the down sampling of the coefficients

Fig 5.1 Block diagram of discrete wavelet transform (DWT)

As in the pyramid algorithm proposed by Mallat [17], the DWT coefficients at an arbitrary level j can be computed from the DWT coefficients of its previous level $j+1$, which is expressed as follows [18]:

$$\mathbf{c}_j(\mathbf{k}) = \sum \mathbf{h}_0(\mathbf{m}-2\mathbf{k}) \mathbf{c}_{j+1}(\mathbf{m})$$

$$\mathbf{d}_j(\mathbf{k}) = \sum \mathbf{h}_1(\mathbf{m}-2\mathbf{k}) \mathbf{c}_{j+1}(\mathbf{m})$$

where c_j and d_j are the scaling coefficient and the wavelet coefficient of level j respectively, whereas $h_0(n)$ and $h_1(n)$ are the dilation coefficients corresponding to the scaling and wavelet functions respectively. The dilation coefficients $h_0(n)$ and $h_1(n)$ are also the coefficients of a low pass and a high pass filter respectively. As a result, the scaling and wavelet coefficients at level j are obtained by filtering the scaling coefficients at level $j+1$ using an analysis quadrature mirror filter bank (QMF). Scaling coefficients at level $j+1$ is obtained by combining the scaling and wavelet coefficients at level j :

$$\mathbf{c}_{j+1}(\mathbf{k}) = \sum \mathbf{c}_j(\mathbf{m}) \mathbf{h}_0'(\mathbf{k}-2\mathbf{m}) + \sum \mathbf{d}_j(\mathbf{m}) \mathbf{h}_1'(\mathbf{k}-2\mathbf{m})$$

Each level of the 2-D DWT operation requires two stages of 1-D DWT operations. First, 1-D DWT is performed on the row data, producing high pass and low pass outputs. A second stage 1-D DWT is executed on the columns of the high pass and low pass outputs of the first stage to obtain four sub-images. Further decomposition can be made on the sub-image in a similar way. In this way, an image is decomposed into a set of sub-images with various resolutions corresponding to the different scales.

5.5 Results and Discussions

The set of 28 samples of stator line voltages and current of induction motor taken under no load condition in healthy as well as faulty condition were down sampled by discrete wavelet transform algorithm and decomposed to 2 level. The decomposed data contains set of 17 samples. The coefficients obtained after the 2 level decomposition is shown in table XII.

Table XII: Detailed and approximation coefficients obtained

Sl no .	Detailed coefficients of voltage samples	Approximation coefficients of voltage samples	Detailed coefficients of current samples	Approximation coefficients of current samples	Detailed coefficients of target output (health condition of insulation)	Approximation coefficients of target output (health condition of insulation)
1	0.2636	93.7186	0.0325	0.4316	0.0000	1.2728
2	0.0270	73.0138	0.0722	0.4637	0.0000	1.2728
3	-0.7251	56.8512	0.0309	1.4957	0.0000	1.2728
4	-1.3878	63.9298	-0.0118	0.8100	0.0000	1.2728
5	1.9192	84.7466	-0.0011	0.4473	0.0000	1.2728
6	-0.1502	100.0156	-0.0048	0.4240	0.0000	1.2728
7	-35.3388	115.5769	0.1907	0.4343	-0.1096	1.2678
8	13.4773	146.1123	-0.0700	0.3673	0.0410	1.3032
9	-34.6124	124.0771	-0.1101	0.5876	0.0070	1.1671
10	3.9437	91.1459	0.0346	0.9949	-0.0568	0.8440
11	-7.0086	87.2534	-0.2368	0.9705	0.1463	0.8124
12	1.1084	46.4532	0.3748	1.6728	-0.2120	0.4064
13	-18.2150	56.3135	0.1245	1.8745	-0.1301	0.2936
14	7.3664	66.7297	0.0483	1.9744	0.0513	0.2521
15	-2.0109	57.9744	-0.0367	0.7971	-0.0086	0.6456
16	-1.1155	36.1638	-0.0616	0.9446	-0.0082	0.5416
17	18.7065	52.7153	-0.2097	1.6162	0.1913	0.5561

5.5.1 Tabulation of approximate RMS error in the coefficients for different l and m obtained from RBFNN

TABLE XIII: Approximate RMS error in the coefficients for $l=0.1$, $m=0.4$ and $m=0.5$

Epoch no.	$l=0.1$ and $m=0.4$		$l=0.1$ and $m=0.5$	
	RMS error in detailed coefficient of target output (healthiness of insulation)	RMS error in approximation coefficient of target output (healthiness of insulation)	RMS error in detailed coefficient of target output (healthiness of insulation)	RMS error in approximation coefficient of target output (healthiness of insulation)
1	0.0320	0.0304	0.0317	0.0307
2	0.0316	0.0298	0.0312	0.0304
3	0.0313	0.0294	0.0308	0.0301
4	0.0311	0.0292	0.0306	0.0299
5	0.0309	0.0289	0.0304	0.0298
6	0.0308	0.0287	0.0302	0.0297
7	0.0307	0.0286	0.0300	0.0295
8	0.0306	0.0284	0.0299	0.0295
9	0.0305	0.0283	0.0298	0.0294
10	0.0304	0.0281	0.0297	0.0293
11	0.0304	0.0280	0.0296	0.0292
12	0.0303	0.0279	0.0295	0.0291
13	0.0302	0.0277	0.0294	0.0291
14	0.0302	0.0276	0.0293	0.0290
15	0.0301	0.0275	0.0293	0.0289
16	0.0301	0.0273	0.0292	0.0288
17	0.0300	0.0272	0.0291	0.0288
18	0.0300	0.0271	0.0291	0.0287
19	0.0299	0.0269	0.0290	0.0286
20	0.0299	0.0267	0.0290	0.0285
21	0.0299	0.0266	0.0289	0.0284
22	0.0298	0.0264	0.0289	0.0283
23	0.0298	0.0262	0.0289	0.0282
24	0.0298	0.0259	0.0288	0.0280
25	0.0298	0.0257	0.0288	0.0279
26	0.0297	0.0254	0.0288	0.0277

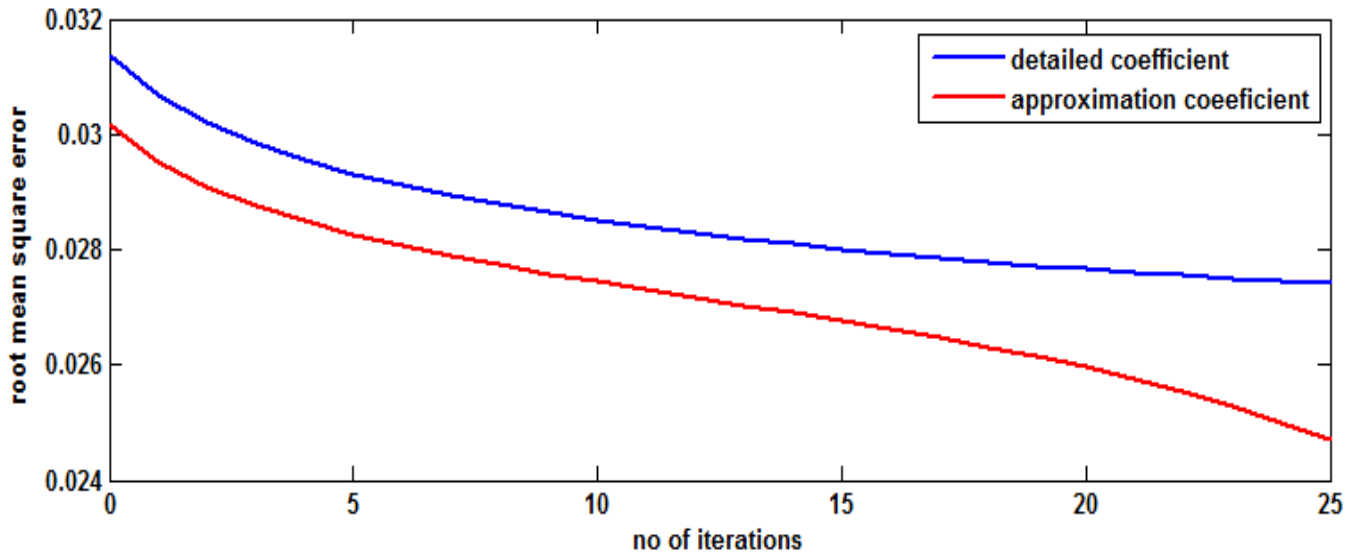


Fig 5.2 RMS error vs. no of iterations in detailed and approximation coefficients of target output for $l=0.1$ and $m=0.4$

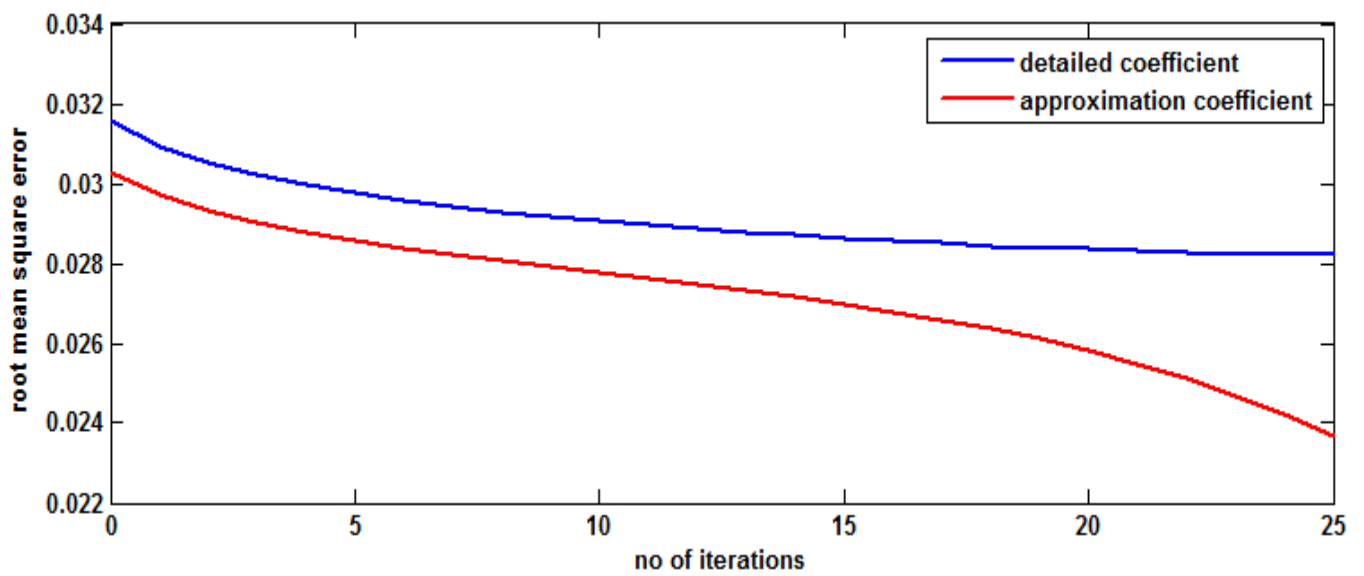


Fig 5.3 RMS error vs. no of iterations in detailed and approximation coefficients of target output for $l=0.1$ and $m=0.5$

TABLE XIV: Approximate RMS error in the coefficients for $m=0.5$, $l=0.2$ and $l=0.3$

Epoch no.	$l=0.2$ and $m=0.5$		$l=0.3$ and $m=0.5$	
	RMS error in detailed coefficient of target output (healthiness of insulation)	RMS error in approximation coefficient of target output (healthiness of insulation)	RMS error in detailed coefficient of target output (healthiness of insulation)	RMS error in approximation coefficient of target output (healthiness of insulation)
1	0.0314	0.0304	0.0317	0.0298
2	0.0307	0.0299	0.0312	0.0290
3	0.0302	0.0296	0.0309	0.0284
4	0.0298	0.0293	0.0306	0.0280
5	0.0295	0.0291	0.0304	0.0277
6	0.0293	0.0289	0.0302	0.0274
7	0.0291	0.0287	0.0301	0.0271
8	0.0289	0.0286	0.0299	0.0269
9	0.0288	0.0284	0.0298	0.0267
10	0.0286	0.0283	0.0297	0.0265
11	0.0285	0.0282	0.0296	0.0263
12	0.0284	0.0281	0.0295	0.0261
13	0.0283	0.0279	0.0295	0.0259
14	0.0282	0.0278	0.0294	0.0257
15	0.0281	0.0277	0.0293	0.0255
16	0.0280	0.0275	0.0293	0.0254
17	0.0279	0.0274	0.0292	0.0252
18	0.0279	0.0272	0.0291	0.0249
19	0.0278	0.0270	0.0291	0.0247
20	0.0277	0.0268	0.0291	0.0245
21	0.0277	0.0266	0.0290	0.0242
22	0.0276	0.0263	0.0290	0.0239
23	0.0276	0.0260	0.0289	0.0236
24	0.0275	0.0257	0.0289	0.0232
25	0.0275	0.0253	0.0289	0.0228
26	0.0275	0.0249	0.0289	0.0224

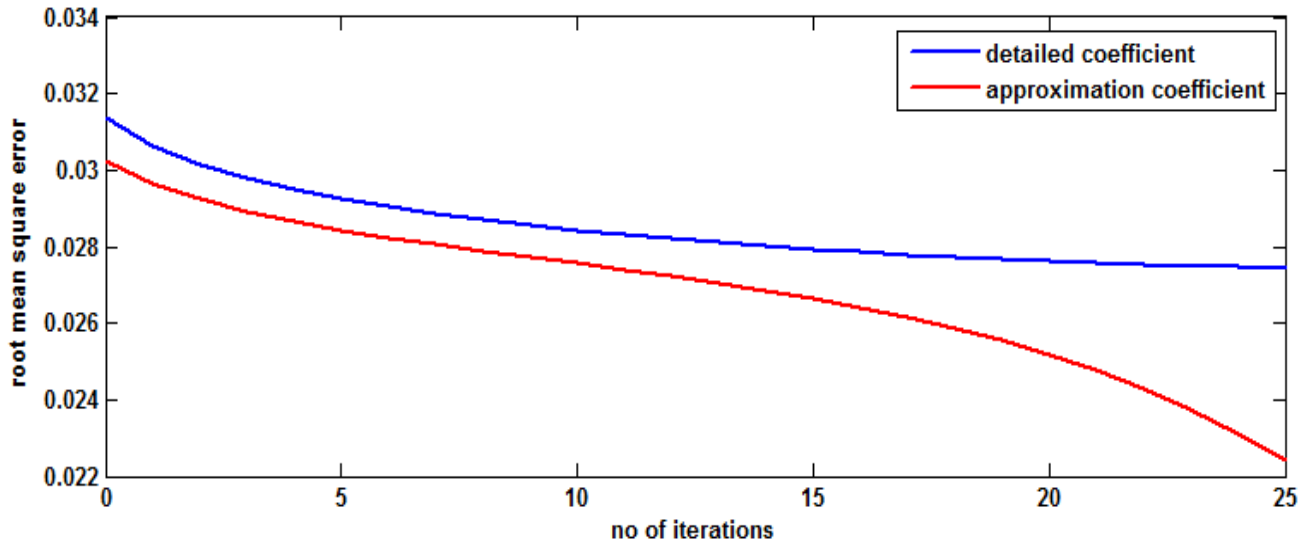


Fig 5.4 RMS error vs. no of iterations in detailed and approximation coefficients of target output for $l=0.2$ and $m=0.5$

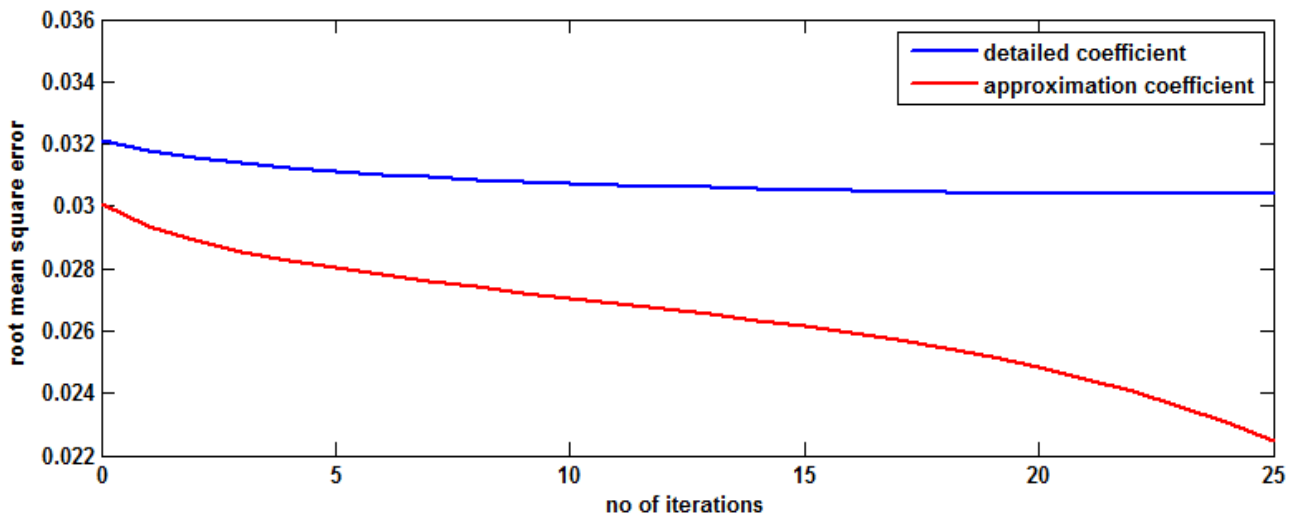


Fig 5.5 RMS error vs. no of iterations in detailed and approximation coefficients of target output for $l=0.3$ and $m=0.5$

TABLE XV: Approximate RMS error in the coefficients for $m=0.4$, $l=0.1$ and $l=0.2$

Epoch no.	$l=0.1$ and $m=0.4$		$l=0.2$ and $m=0.4$	
	RMS error in detailed coefficient of target output (healthiness of insulation)	RMS error in approximation coefficient of target output (healthiness of insulation)	RMS error in detailed coefficient of target output (healthiness of insulation)	RMS error in approximation coefficient of target output (healthiness of insulation)
1	0.0320	0.0304	0.0315	0.0302
2	0.0316	0.0298	0.0309	0.0296
3	0.0313	0.0294	0.0304	0.0292
4	0.0311	0.0292	0.0301	0.0289
5	0.0309	0.0289	0.0299	0.0286
6	0.0308	0.0287	0.0296	0.0284
7	0.0307	0.0286	0.0295	0.0282
8	0.0306	0.0284	0.0293	0.0280
9	0.0305	0.0283	0.0292	0.0279
10	0.0304	0.0281	0.0290	0.0277
11	0.0304	0.0280	0.0289	0.0276
12	0.0303	0.0279	0.0288	0.0275
13	0.0302	0.0277	0.0287	0.0273
14	0.0302	0.0276	0.0286	0.0272
15	0.0301	0.0275	0.0285	0.0271
16	0.0301	0.0273	0.0285	0.0269
17	0.0300	0.0272	0.0284	0.0268
18	0.0300	0.0271	0.0283	0.0266
19	0.0299	0.0269	0.0283	0.0265
20	0.0299	0.0267	0.0282	0.0263
21	0.0299	0.0266	0.0281	0.0261
22	0.0298	0.0264	0.0281	0.0259
23	0.0298	0.0262	0.0280	0.0257
24	0.0298	0.0259	0.0280	0.0255
25	0.0298	0.0257	0.0280	0.0252
26	0.0297	0.0254	0.0279	0.0249

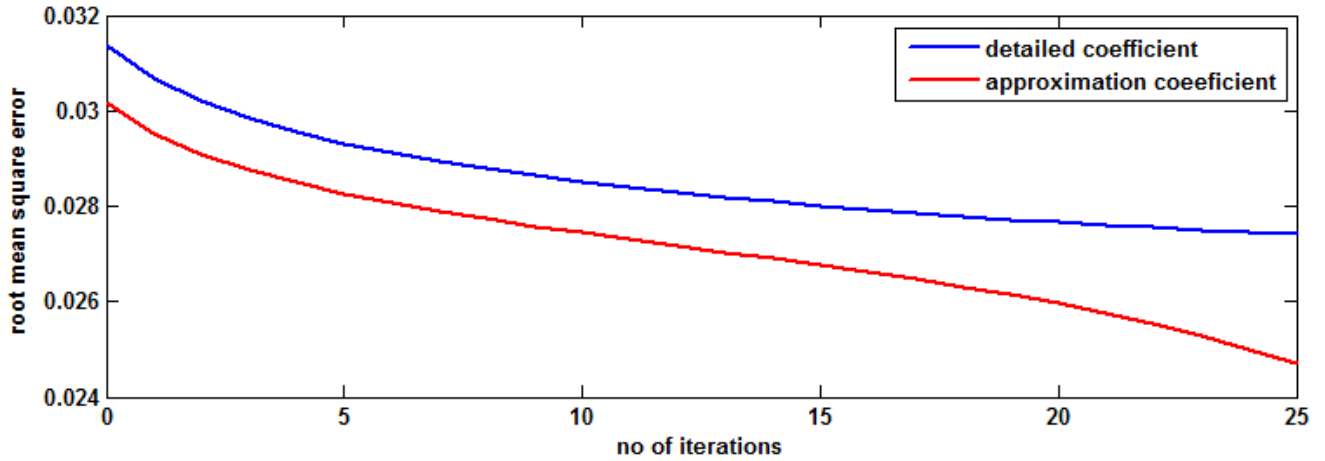


Fig 5.6 RMS error vs. no of iterations in detailed and approximation coefficients of target output for $l=0.1$ and $m=0.4$

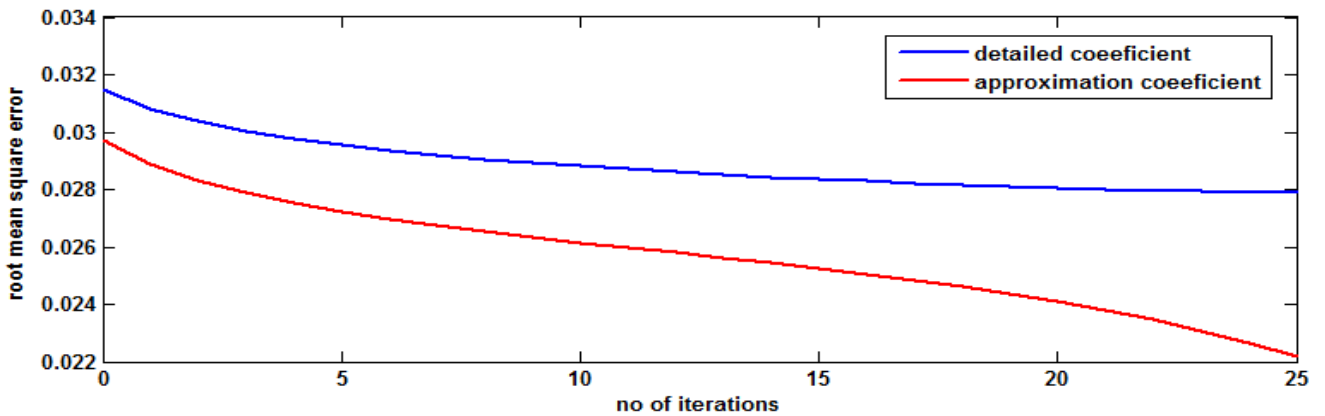


Fig 5.7 RMS error vs. no of iterations in detailed and approximation coefficients of target output for $l=0.2$ and $m=0.4$

5.6 Chapter Summary

In this chapter, the discrete wavelet transform is implemented to diagnose the stator inter-turn short circuit fault of an induction motor. The stator line voltages and current are used as input data for the analysis of stator insulation condition under both healthy and faulty condition. By using the discrete wavelet transform the approximation and detailed coefficients corresponding to the insulation condition of the motor are obtained. From these coefficients the severity of the fault condition can be determined.

Chapter 6

Conclusions and Suggestions for Future Work

6.1 Conclusions of the Thesis

This thesis presents an experimental setup for the measurement of induction motor parameters such as stator current, stator line voltages and rotor speed both under healthy and stator inter-turn short circuit fault conditions. For these measurements we have applied variac voltage varied in steps from 40-115 V under both healthy and shorting the stator winding for every two turns sequentially, beginning with turn '1' and ending with turn 710 of the induction motor. Then different neural network techniques such as BPA and RBFNN are used for the diagnosis of stator inter-turn short circuit fault of the induction motor. It explains each technique clearly using flow chart and training methodology used. It describes the commonly used radial basis functions and the typical RBF used in this thesis for the determination of the healthy condition of the induction motor insulation.

We see that Radial Basis Function Neural Network requires very little memory for approximation and also gets trained very fast with fewer number of training data examples. When for a given set of training data Back Propagation Algorithm requires 500 epoch Radial Basis Function Neural Network requires only 25 or less number of epoch as seen in figure 4.7, 4.8, 4.9, 4.10, 4.11 and 4.12. Also the root mean square in case of Radial Basis Function Neural Network is far less than in case of Back Propagation Algorithm so we can conclude that Radial Basis Function Neural Network is better approximation method and more efficient than Back Propagation Algorithm.

Lastly the discrete wavelet transform is implemented to diagnose the stator inter-turn short circuit fault of an induction motor. The stator line voltages and current are used as input data for the analysis of stator insulation condition under both healthy and faulty condition. By using the discrete wavelet transform the approximation and detailed coefficients corresponding to the insulation condition of the motor are obtained. From these coefficients the severity of the fault

condition is determined.

Finally we compare the RMS error obtained in all the three above techniques used for the fault diagnosis of induction motor as shown in table below.

Table XVI: RMS error in case of BPA, RBFNN and DWT

EPOCH No.	BPA	RBFNN	DWT Detailed coefficients	DWT Approximation coefficients
1	0.1014	0.0142	0.0303	0.0279
2	0.0959	0.0141	0.0302	0.0277
3	0.0931	0.0140	0.0302	0.0276
4	0.0916	0.0140	0.0301	0.0275
5	0.0905	0.0138	0.0301	0.0273
6	0.0897	0.0135	0.0300	0.0272
7	0.0888	0.0126	0.0300	0.0271
8	0.0880	0.0120	0.0299	0.0269
9	0.0872	0.0122	0.0299	0.0267
10	0.0865	0.0132	0.0299	0.0266
11	0.0857	0	0.0298	0.0264
12	0.0850	0	0.0298	0.0262
13	0.0843	0	0.0298	0.0259
14	0.0836	0	0.0298	0.0257
15	0.0829	0	0.0297	0.0254

So we see that RBFNN outperforms BPA and DWT.

6.2 Thesis Contributions

The following are the contributions of the thesis.

- Development of an experimental setup for measuring the induction motor stator line voltages and current and rotor speed under both healthy and short circuit conditions.
- Application of different artificial neural network techniques for the fault diagnosis of the 2 hp induction motor such as back propagation algorithm (BPA) and radial basis function neural network (RBFNN).

- Using discrete wavelet transform to predict the health condition of insulation of the stator winding of the 2 hp induction motor.

6.3 Future scope of work

In this work, artificial neural networks like BPA and RBFNN were used for the stator inter turn fault diagnosis of induction motor.

- The same networks can be applied for the identification and location of the other faults such as bearing fault, rotor broken bar fault, and eccentricity related fault of an induction motor.
- DWT can be used for detection of several other stator and rotor related faults in induction machine based on current signature and vibrations of the machine.
- Neural system troupes are accepting expanding consideration in the field of examination such as control, issue finding, choice making, and recognizable proof, apply autonomy and so forth because of their learning and speculation capacities, nonlinear mapping, and parallelism of calculation. In any case, for tackling issue location issues the neural systems may get stuck on a nearby least of the lapse surface, and the system joining rate is by and large moderate. A suitable methodology for defeating these weaknesses is the utilization of wavelet capacities in the system structure. Wavelet capacity is a waveform that has restricted length of time and a normal estimation of zero. A wavelet neural system has a nonlinear relapse structure that utilizations limited premise works in the shrouded layer to attain to the data yield mapping. The coordination of the restriction properties of wavelets and the learning capacities of neural system brings about the upsides of wavelet neural system over neural system for the discovery and area of inter turn short out issue in the stator winding of an induction machine.

References

- [1] MO-yuen Chow, Member, IEEE, Peter M. Mangum, Member, IEEE, and Sui Oi Yee, Student Member, (1991), A Neural Network Approach to Real-Time Condition Monitoring of Induction Motors, IEEE Transactions on Industrial Electronics, VOL. 38, NO. 6, December 1991
- [2] Mo-yuen Chow, Paul V. Goode(1993), Adaptation of a Neural/Fuzzy Fault Detection System, Dept. of Electrical and Computer Engineering, North Carolina State University, Raleigh, NC 27695-7911
- [3] B K BOSE (1994), Expert System, Fuzzy Logic, and Neural Network Applications in Power Electronics and Motion Control, 1994
- [4] James E. Timperley (1983), Incipient Fault Identification through Neural RF Monitoring of large rotating machines, IEEE Transactions on Power Apparatus and Systems, Member IEEE American Electric Power Service Corporation, Canton, Ohio 44701, Vol. PAS-102, No. 3, March 1983
- [5] W. Thomson and M. Fenger, Current Signature Analysis to Detect Induction Motor Faults, IEEE Ind. Appl. Mag., vol. 7, no. 4, pp. 26–34, 2001.
- [6] H. Nejjari, M. H. Benbouzid, “Monitoring and Diagnosis of Induction Motors Electrical Faults using a Current Park’s Vector Pattern Learning Approach, IEEE Trans. Ind. Appl., vol. 36, no. 3, 2000.
- [7] Sanner, R.M., Slotine, J.J.E., (1994), “Gaussian network for direct adaptive control”, IEEE Transaction on Neural Networks, vol.3, no 6, pp.837-863
- [8] Haykin, Neural Networks: A Comprehensive Foundation, 1994
- [9] Yousef Akhlaghi, Radial Basis Function Networks

- [10] H.A. Talebi and Farzaneh Abdollahi (Department of Electrical Engineering), Amirkabir University of Technology, Lecture 4: Neural Networks, Radial Basis Function Networks
- [11] Filippetti, G. Franceschini, and C. Tassoni, "Recent Developments of Induction Motor Drives Fault Diagnosis Using AI Techniques," *IEEE Trans. Ind. Electron.*, vol. 47, no. 5, pp. 994–1003, 2000.
- [12] Zhe-Lee Gaing, IEEE Member, "Wavelet-Based Neural Network for Power Disturbance Recognition and Classification."
- [13] XIAN-XIANG LI, QIAN-JIN ZHANG and HONG-JUN XIAO, "The Design of brushless DC motor servo system based on wavelet ANN"
- [14] A. Siddique and G. S. Yadava, "A Review of Stator Fault Monitoring Techniques Of Induction Motors," *IEEE Trans. Energy Convers.*, vol. 20, no. 1, pp. 106–114, 2005
- [15] V. Wowk, *Machinery Monitoring. Machinery Vibration- Measurement and Analysis* (pp. 17-18). New York: McGraw-Hill Inc.
- [16] N. Neale, *Condition Monitoring Methods and their Interpretation. A guide to the condition monitoring of machines* (pp. 50-89). London: department of trade and industry press, 1980.
- [17] S.G. Mallat, "A Theory of multiresolution signal decomposition: The wavelet representation", *IEEE Trans. on Pattern Recognition and Machine Intelligence*. Vol. 11, Jul. 1989.
- [18] Yong Liu and Edmund M-K. Lai, Senior Member, IEEE, 'Design and Implementation of an RNS-Based 2-D DWT Processor', *IEEE Transactions on Consumer Electronics*, Vol. 50, No. 1, FEBRUARY 2004